Chem Soc Rev

Chemical Society Reviews

www.rsc.org/chemsocrev

Volume 37 | Number 12 | December 2008 | Pages 2581–2800

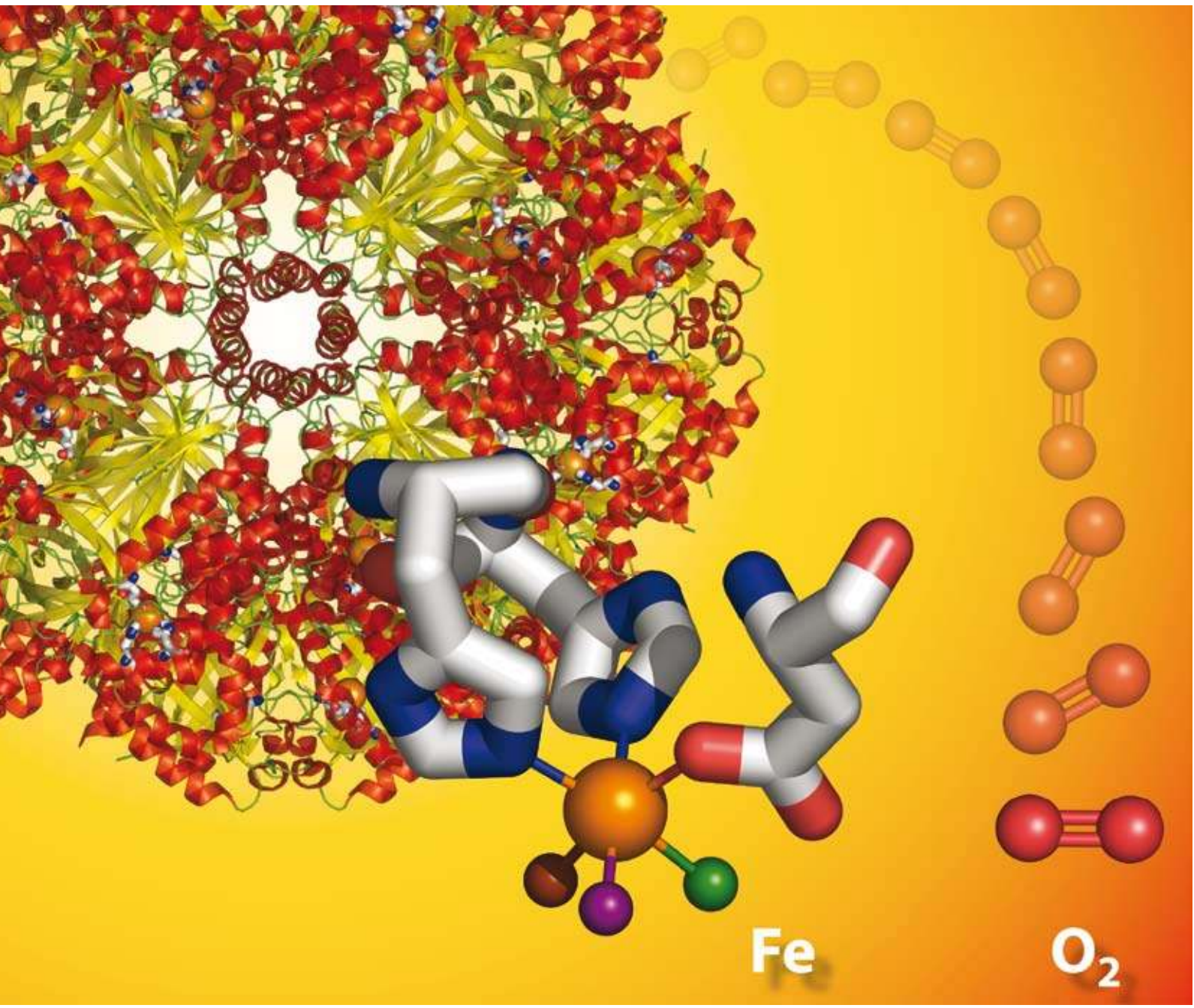

ISSN 0306-0012

CRITICAL REVIEW
Robertus J. M. Klein Gebbink *et al.*
Mononuclear non-heme iron enzymes with the 2-His-1-carboxylate facial triad: recent developments in enzymology and modeling studies

TUTORIAL REVIEW
Yoshio Okamoto and Tomoyuki Ikai
Chiral HPLC for efficient resolution of enantiomers

RSC Publishing

Mononuclear non-heme iron enzymes with the 2-His-1-carboxylate facial triad: recent developments in enzymology and modeling studies

Pieter C. A. Bruijnincx, Gerard van Koten and Robertus J. M. Klein Gebbink*

Received 25th June 2008
First published as an Advance Article on the web 14th October 2008
DOI: 10.1039/b707179p

Iron-containing enzymes are one of Nature's main means of effecting key biological transformations. The mononuclear non-heme iron oxygenases and oxidases have received the most attention recently, primarily because of the recent availability of crystal structures of many different enzymes and the stunningly diverse oxidative transformations that these enzymes catalyze. The wealth of available structural data has furthermore established the so-called 2-His-1-carboxylate facial triad as a new common structural motif for the activation of dioxygen. This superfamily of mononuclear iron(II) enzymes catalyzes a wide range of oxidative transformations, ranging from the *cis*-dihydroxylation of arenes to the biosynthesis of antibiotics such as isopenicillin and fosfomycin. The remarkable scope of oxidative transformations seems to be even broader than that associated with oxidative heme enzymes. Not only are many of these oxidative transformations of key biological importance, many of these selective oxidations are also unprecedented in synthetic organic chemistry. In this *critical review*, we wish to provide a concise background on the chemistry of the mononuclear non-heme iron enzymes characterized by the 2-His-1-carboxylate facial triad and to discuss the many recent developments in the field. New examples of enzymes with unique reactivities belonging to the superfamily have been reported. Furthermore, key insights into the intricate mechanistic details and reactive intermediates have been obtained from both enzyme and modeling studies. Sections of this review are devoted to each of these subjects, *i.e.* the enzymes, biomimetic models, and reactive intermediates (225 references).

1. Introduction

The oxidation of organic compounds is thermodynamically downhill and large amounts of energy are released in these reactions. However, the ground state of dioxygen in the atmosphere is open-shell, triplet O_2 and the (concerted) reaction of organic substrates, which usually have a singlet ground state, with dioxygen is a spin-forbidden process.[1] On a positive note, this means that spontaneous combustion of organic material, *i.e.* all forms of life, to carbon dioxide and water is prevented. Another consequence of the spin mismatch and the low one-electron oxidation potential of triplet oxygen is its rather sluggish kinetic reactivity.[2]

Nature has evolved an elegant solution to overcome the kinetic barrier for the activation of dioxygen by using *e.g.* transition metals. More specifically, several metalloenzymes

Chemical Biology & Organic Chemistry, Department of Chemistry, Debye Institute for Nanomaterials Science, Faculty of Science, Utrecht University, Padualaan 8, 3584 CH Utrecht, The Netherlands. E-mail: r.j.m.kleingebbink@uu.nl

Pieter Bruijnincx

Pieter Bruijnincx obtained his PhD degree (cum laude) in 2007 from Utrecht University under the guidance of Profs. Bert Klein Gebbink, Gerard van Koten, and Bert Weckhuysen. Currently, he is a Rubicon postdoctoral fellow in the group of Prof. Peter Sadler at the University of Warwick, working on new strategies for ruthenium anticancer drugs.

Gerard van Koten

Gerard van Koten has been Professor of Organic Chemistry and Catalysis at Utrecht University since 1986 and became Distinguished Professor of Utrecht University in 2004. Since 2005 he has acted as Dean of the Faculty of Science at Utrecht University and in 2007 also became part-time research professor at Cardiff University. His research interests comprise the study of fundamental processes in organometallic chemistry and the application of organometallic complexes as homogeneous catalysts.

catalyze the controlled and selective oxidation of organic compounds. The geometry and structural features of the active site and the choice of incorporated metal are very diverse and fully optimized to the function of the protein or enzyme. Establishing the correlation of the geometric and electronic structure with function is one of the main objectives of the field of bioinorganic chemistry.[2,3] The activation of dioxygen on metal sites requires the availability of different redox states. Metalloenzymes capable of dioxygen activation consist mainly of enzymes with copper or iron active sites.[4,5] A wide variety of different mono- or multinuclear iron and copper enzymes have been discovered and found to catalyze major biological transformations.

The iron-containing enzymes that are involved in dioxygen activation can be divided into two groups based on the active site structures, *i.e.* heme and non-heme containing enzymes. The heme enzymes have been studied extensively and are well understood, with cytochrome P450 as the prototypical example.[6] The non-heme iron enzymes can in turn be divided in mononuclear and dinuclear iron enzymes.[2,7,8] Methane monooxygenase, for instance, is a remarkable example of the latter group and catalyzes the selective oxidation of the most difficult of hydrocarbon substrates, *i.e.* the oxidation of methane to methanol.[8]

Yet, the mononuclear non-heme iron oxygenases have received the most attention recently, primarily because of the recent availability of crystal structures of many different enzymes and the stunningly diverse oxidative transformations that these enzymes catalyze.[1,7,9] The wealth of structural data has furthermore established a new common structural motif for the activation of dioxygen.[9] This structural motif consists of a mononuclear iron(II) metal center that is coordinated facially by two histidine residues and one carboxylato ligand from either a glutamate or aspartate residue (Fig. 1). This structural motif has been coined the '2-His-1-carboxylate facial triad'.[10,11]

The superfamily of non-heme iron enzymes with this 2-His-1-carboxylate facial triad will be the focus of this review. Several excellent reviews have been devoted (partly) to these enzymes,[1–3,7,9,12] and address the structural aspects of the enzymes, spectroscopic and theoretical methods and modeling studies. An excellent highlight on the versatility in oxygen activation reactions of biological non-heme Fe(II) centers has also recently appeared.[13] Here, we provide a concise background and discuss the recent developments. Indeed, several new discoveries and important advances have appeared since the publication of the comprehensive review by Que and co-workers at the beginning of 2004.[7] Several new examples of enzymes with unique reactivities belonging to the superfamily have been reported since. In addition, more insight into the mechanistic details and reactive intermediates has been obtained from both enzyme and modeling studies. Sections of this review are devoted to each of these subjects, *i.e.* the enzymes, models, and reactive intermediates.

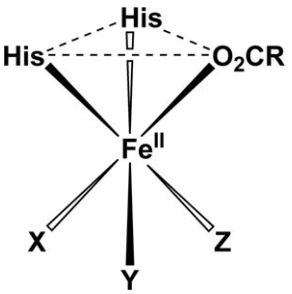

Fig. 1 Schematic representation of the 2-His-1-carboxylate facial triad (X, Y and Z denote weakly bound solvent molecules or vacant sites).

2. The 2-His-1-carboxylate facial triad: general aspects

Over the last 10 years, there has been an explosion of available crystal structures of non-heme iron enzymes. The 2-His-1-carboxylate facial triad has thus been established in over 30 different, structurally characterized enzymes.[9] The active site triad of this superfamily of enzymes can thus be regarded as one of Nature's recurring motifs, like the heme cofactor and iron–sulfur clusters.[11] It is interesting to note that the primary sequence homology amongst the different subfamilies (*vide infra*) is low. This implies that the triad is the result of a convergent evolution of unrelated enzymes and that this particular coordination geometry and choice of metal is inherently favored for different oxidative transformations.[7]

The structural features of the 2-His-1-carboxylate facial triad are exemplified by the resting state of deacetoxycephalosporin C synthase (DAOCS), an enzyme that catalyzes the ring expansion of the thiazolidine ring of penicillin N to afford deacetoxycephalosporin C (Fig. 2).[9,14] One face of the octahedral coordination sphere of the ferrous metal center is occupied by three endogenous ligands, *i.e.* two histidines and one aspartate or glutamate residue. The enzyme thus provides the divalent metal center with a well-suited, monoanionic platform. In the as-isolated state of the enzymes, the other three coordination sites usually are either occupied by weakly bound and easily displaceable solvent molecules or are vacant. These three sites are therefore readily available for the binding of dioxygen, substrates, and cofactors. This flexibility in coordination chemistry at the metal seems the primary reason for the observed diversity in catalyzed oxidative transformations.[7] Small variations in the triad have been observed, such

Bert Klein Gebbink

Bert Klein Gebbink obtained his PhD degree from Nijmegen University in 1998 under the guidance of Prof. Roeland Nolte. After a postdoctoral stay at Stanford University (Prof. Dan Stack), he joined the Van Koten group at Utrecht University as a postdoc and later assistant and associate professor. Presently, he holds a personal chair in 'Synthetic and Biological Chemistry of Transition Metal Complexes' at Utrecht University.

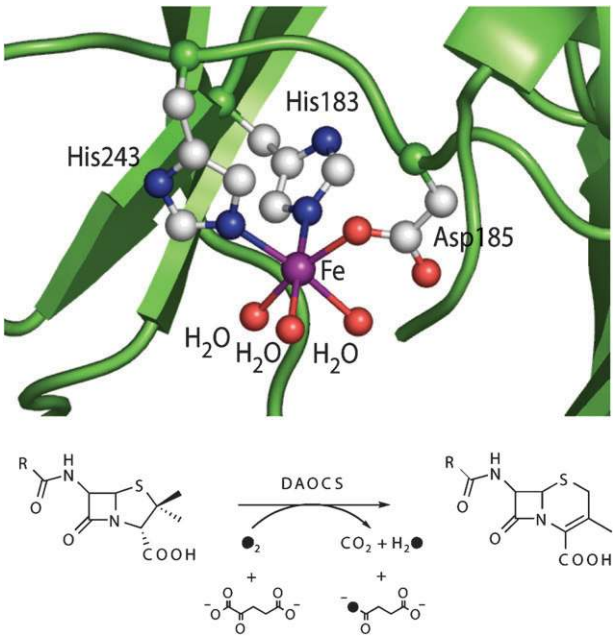

Fig. 2 The active site of deacetoxycephalosporin C synthase (DAOCS) features the 2-His-1-carboxylate facial triad (protein database accession code: 1RXF.pdb) (top). DAOCS catalyzes the ring expansion of the thiazolidine ring of penicillin N to afford deacetoxycephalosporin C (bottom).[16]

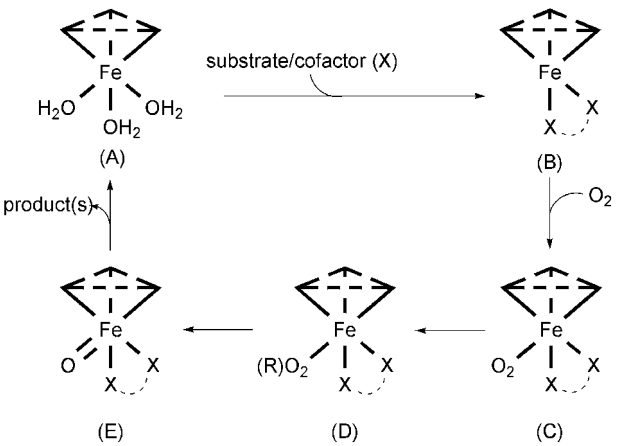

Fig. 3 General mechanistic pathway for reactions catalyzed by the 2-His-1-carboxylate facial triad superfamily of non-heme iron(II) enzymes. Picture adapted from Que and co-workers.[9]

as a bidentate coordination of the carboxylato group in some of the Rieske oxygenases, amongst others.[7,15] For these enzymes, two vacant sites are available for substrate, cofactor and/or dioxygen binding. In this case, the coordination of the metal ion by the three endogenous residues cannot be strictly called facial and is therefore referred to as '2-His-1-carboxylate structural motif' in these particular cases.

Although the superfamily of enzymes catalyzes a very diverse set of reactions, some common mechanistic features are shared by all members (Fig. 3).[2,3,7,9] First, the typically six-coordinate resting state of the enzyme is rather unreactive towards dioxygen (A). The subsequent binding of substrate or cofactor results in the formation of a coordinatively unsaturated, five-coordinate metal center, which greatly enhances its dioxygen affinity (B).[3] This coupling of reactivity with substrate binding is a protection mechanism for the enzyme against self-inactivation. In the next step, dioxygen is activated for reaction by direct binding to the metal center (C). The enzymes use two different ways of activating dioxygen and overcome the low one-electron redox potential of dioxygen by acquiring additional reducing equivalents from either a redox-active cofactor or a redox-active substrate.[3] The flexibility of the triad allows the binding of dioxygen *trans* to any of the three endogenous residues and the different *trans*-effects have been suggested to modulate the reactivity of the enzyme.[9,11] Dioxygen is then reduced to the peroxide level (D) and from this point on the proposed mechanisms for the different enzymes diverge. In most cases O–O bond cleavage and the formation of a high-valent iron–oxo species is invoked (E). This iron–oxo species, be it Fe(IV) or Fe(V), is proposed to be the actual oxidizing species. The assignment of the structure of the oxidizing species is tentative in most cases, but has precedence in both modeling and enzyme studies. Direct evidence for a high-valent iron–oxo species has for instance been reported for the α-ketoglutarate-dependent enzymes taurine/α-ketoglutarate dioxygenase (TauD),[17–20] prolyl-4-hydroxylase (P4H),[21] and the related halogenase CytC3.[22] Several biomimetic oxoiron(IV)[23–25] complexes and, very recently, an oxoiron(V) species[26] have also been characterized. Alternatively, an iron(III)–superoxide species has been suggested as the oxidizing species in, for instance, isopenicillin *N* synthase (IPNS). In this particular case, the thiolate-bound substrate stabilizes the formation of an end-on superoxide and prevents the formation of the generally invoked dioxygen bridged binding and subsequent formation of a high-valent iron–oxo species, thus steering the reactivity of the enzyme from oxygenase to oxidase.[27]

3. The 2-His-1-carboxylate facial triad: enzyme groups

The enzymes featuring the 2-His-1-carboxylate facial triad can be classified into five different groups based on their structural characteristics, reactivity, and specific requirements for catalysis. These groups are the (1) extradiol cleaving catechol dioxygenases, (2) Rieske oxygenases, (3) α-ketoglutarate-dependent enzymes, (4) pterin-dependent hydroxylases, and finally (5) a miscellaneous, catch-all category. The basic characteristics, recent developments, and illustrative examples of each group will be discussed.

3.1 Extradiol cleaving catechol dioxygenases

Oxidative ring cleavage is a key metabolic step in the biodegradation of aromatic compounds by bacteria.[28] The common metabolic pathway is ring fission of catecholic substrates, which is catalyzed by the extradiol cleaving catechol dioxygenases.[2,7,28,29] These enzymes utilize a non-heme iron(II) active site (or in a few cases Mn(II))[30] to cleave the C–C bond next to the two hydroxyl groups with incorporation of both atoms of dioxygen in the substrate (Fig. 4). Alternatively, their intradiol cleaving catechol dioxygenase counterparts, which

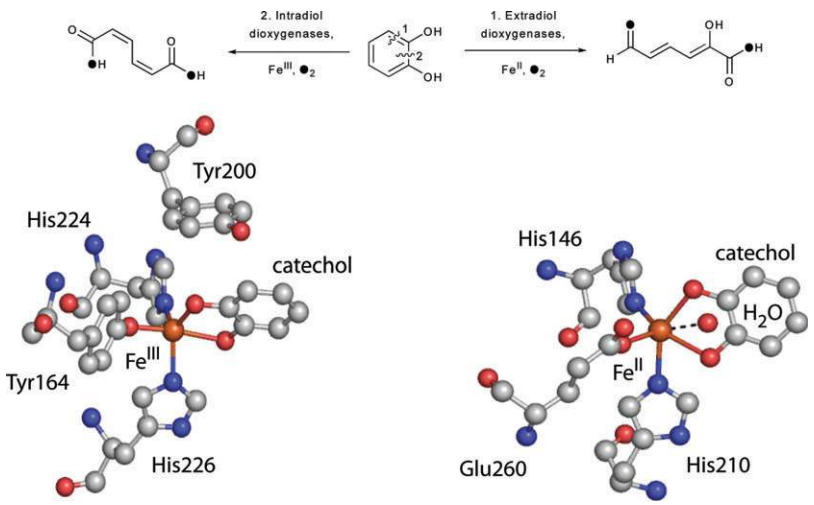

Fig. 4 Top: The extradiol and intradiol catechol cleavage pathways catalyzed by the respective catechol cleaving dioxygenases. Bottom: Enzyme–substrate (catechol) complexes of the extradiol enzyme 2,3-dihydroxybiphenyl 1,2-dioxygenase (right, 1KND.pdb) and the intradiol enzyme catechol 1,2-dioxygenase (left, 1DLT.pdb).

represent a minor pathway, utilize a non-heme iron(III) active site to cleave the C–C bond in between the two hydroxyl groups of the catechol substrate. The extradiol cleaving dioxygenases are the more versatile of the two groups of enzymes and in addition to catecholic substrates also accept gentisate, salicylate, hydroquinone and 2-aminophenol as substrate.[28] The biological ins-and-outs of the catechol cleaving dioxygenases have been very recently reviewed comprehensively.[28]

Three evolutionary independent classes of extradiol enzymes have been identified which all share similar active sites featuring the 2-His-1-carboxylate facial triad and utilize a similar catalytic strategy.[28] The general reaction mechanism proposed for the extradiol cleaving catechol dioxygenases is outlined in Fig. 5. In the resting state (Fig. 5A), the coordination geometry around the iron is a well-defined square pyramid, with one histidine residue as the axial ligand, and the two other endogenous residues and two water molecules as the equatorial ligands in the basal plane.[28,31] In the first step of the reaction, the substrate displaces the two solvent molecules and binds to the metal to form the five-coordinate enzyme-substrate complex (Fig. 4, bottom right).[3]

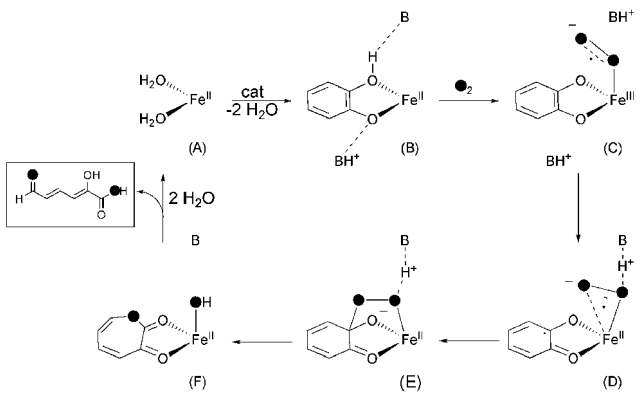

Fig. 5 Proposed mechanism for the extradiol type cleavage of catechols (cat). B depicts a conserved second sphere residue. The ligands of the facial triad have been omitted for clarity.

The substrate binds as a monoanion in an asymmetric fashion[31] and substrate binding greatly enhances the affinity of the metal center for dioxygen (Fig. 5B).[3,32] The dioxygen binding results in two subsequent electron transfer steps. First, an iron(III)–superoxide species is formed by one-electron transfer from the metal to dioxygen (C) and in a second step an electron is transferred from the substrate to the metal to form a semiquinonatoiron(II)–superoxide species (D).[7] In the next step, a proximal alkylperoxo intermediate is formed (E), which undergoes a Criegee rearrangement (alkenyl migration) to form a seven-membered lactone species and a metal bound hydroxide (F). The latter hydrolyzes the lactone and the ring-opened product is formed.

Although the asymmetric binding of the substrate to the iron has been well demonstrated by both spectroscopic and structural studies,[7,28,29,31] up until very recently much less was known about the subsequent steps involving the binding of dioxygen. Evidence for the involvement of a semiquinone species had been obtained from the observation of epimerization of a radical probe substrate analogue[33] in experiments on the enzyme 3-(2′,3′-dihydroxyphenyl)propionate 1′,2′-dioxygenase.[33] Furthermore, transient kinetic studies on homoprotocatechuate 2,3-dioxygenase (2,3-HPCD) using the alternative, less reactive substrate 4-nitrocatechol allowed for the first detection of discrete intermediates in the catalytic cycle.[34] Specific mutants of the native enzyme even allowed the experimental detection of the initial dioxygen adduct.[35] A hybrid DFT study of the catalytic mechanism of the extradiol dioxygenases also corroborated the key steps of the proposed mechanism.[36]

In a recent landmark contribution, Kovaleva and Lipscomb reported direct evidence for three intermediates of the mechanistic cycle.[37] Remarkably, an X-ray crystal structure determination of a crystal of 2,3-HPCD soaked in the slow substrate 4-nitrocatechol that was exposed to an O_2 atmosphere, revealed the structure of a superoxo, an alkylperoxo and a bound product intermediate in the different subunits of a single homotetrameric enzyme molecule (Fig. 6). Rather

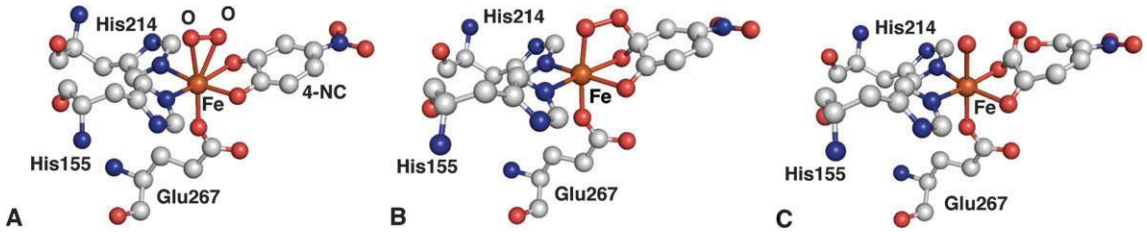

Fig. 6 Structures of the trapped superoxo (A), alkylperoxo (B) and bound product (C) intermediates found in different subunits of homotetrameric 2,3-HPCD during the reaction with slow substrate 4-nitrocatechol (4-NC) and dioxygen in the crystal (2IGA.pdb).[37]

surprisingly, the superoxo intermediate has the O_2 ligand bound side-on (Fig. 6A), rather than the edge-on orientation expected from earlier NO experiments.[37] A second key observation in the superoxo structure is the puckering of the 4-nitrocatechol ring indicating a more sp^3 hybridized carbon atom, consistent with the formulation of the substrate as a semiquinone radical species in this step of the reaction. Two other subunits show the anticipated, but never before characterized bridged iron–alkylperoxo intermediate which results from the recombination of the superoxo and semiquinone radicals (Fig. 6B). Finally, the last subunit contains the ring opened product still bound to the metal center (Fig. 6C). The structural characterization of these reactive intermediates not only provides experimental evidence for key steps in the mechanism of the extradiol type catechol cleavage, it also, in a more general sense, gives credence to the oxygen-activation paradigm for the non-heme iron enzymes with the 2-His-1-carboxylate facial triad.

The origin of the respective regioselectivities of the extradiol and intradiol cleaving catechol dioxygenases is not yet completely understood and is the subject of current research. Intriguingly, a similar proximal alkylperoxo intermediate is proposed in the catalytic cycle of the intradiol cleaving enzymes, albeit with a different iron oxidation state. In the case of intradiol cleavage, however, a different Criegee rearrangement would lead to the formation of an anhydride instead of a lactone. Several different explanations have been offered for the observed difference in regiochemistry.[7,28,29,36] A structural feature of the extradiol dioxygenases that is thought to be essential for the observed regioselectivity is the acid–base chemistry of some conserved second-sphere residues. Structural, theoretical and mutagenesis studies, for instance, suggested that a second-sphere histidine residue acts as a proton donor, which is assumed to protonate the proximal oxygen atom of the alkylperoxo intermediate. DFT studies showed that this protonation step is decisive for the regioselectivity of the reaction.[36] Indeed, substitution of this particular residue resulted in significant changes in reactivity, *i.e.* reduced or complete loss of extradiol cleavage[38,39] and a change in product selectivity.[35,40] The recent crystal structures of the intermediates trapped in 2,3-HPCD also show that conserved histidine His200 is particularly well-positioned to play the role of proton donor.[37]

3.2 Rieske oxygenases

A common first step in the biodegradation of aromatic compounds is their conversion into *cis*-dihydroxylated metabolites. The Rieske non-heme iron dioxygenases catalyze this *cis*-dihydroxylation of arenes regio- and stereospecifically.[7,15] From an environmental point of view aromatic hydrocarbons are common contaminants of soil and groundwater and the Rieske dioxygenases provide an attractive way of biodegradation of these pollutants.[41] Biphenyl dioxygenase has for instance been found to oxidize highly toxic polychlorinated biphenyls and by evolutionary engineering the substrate scope of these enzymes has even been extended to such toxins as dioxin and chlorinated ethenes.[42] Also, a Rieske dioxygenase from a *Sphingomonas* strain and the Rieske dioxygenase biphenyl 2,3-dioxygenase from *Sphingobium yanoikuyae* B1 were shown to be both capable of the degradation of several different polycyclic aromatic hydrocarbons, including the well-known carcinogens chrysene, benzo[*a*]pyrene and benz[*a*]-anthracene.[43,44] This, together with the fact that there is little precedent for its unique reactivity in synthetic organic chemistry,[7,45] has spurred a widespread interest in this group of enzymes. Some Rieske oxygenases have furthermore been shown to be very versatile. Next to *cis*-dihydroxylation, other oxidations such as monohydroxylation, desaturation, sulfoxidation, O- and N-dealkylation, and amine oxidation are also catalyzed.[7,46–49] Examples of some selected reactions catalyzed by Rieske oxygenases are shown in Fig. 7.

The Rieske oxygenases are multicomponent enzymes and consist of a reductase, an oxygenase, and in some cases a ferredoxin component. Substrate oxidation takes place in the oxygenase component, which contains both a Rieske-type [2Fe–2S] cluster and the mononuclear non-heme iron active site. In a single subunit, the Rieske cluster and the non-heme iron center are too far apart to allow for electron transfer ($\sim$45 Å). However, the quaternary structure (trimeric of the $\alpha_3\beta_3$ or α_3 type with three-fold symmetry) allows for electron transfer from a Rieske cluster to a mononuclear iron center from another subunit, which are $\sim$12 Å apart. A key role in the electron transfer has been ascribed to a fully conserved aspartic acid residue that bridges between the two metal sites. Substitution of this aspartate by other amino acids resulted in greatly diminished or even loss of catalytic activity.[15,50,51] For the full reduction of dioxygen two electrons are provided by the substrate and the two additional electrons, supplied by NAD(P)H, are shuttled *via* the reductase or ferredoxin to the Rieske cluster of the oxygenase unit. The cluster in turn passes them on to the non-heme iron active site. Although recently new structural data has become available (*vide infra*), the structural data on the oxygenase component of Rieske oxygenases has long been limited to the crystal structure of the most-studied system, naphthalene dioxygenase

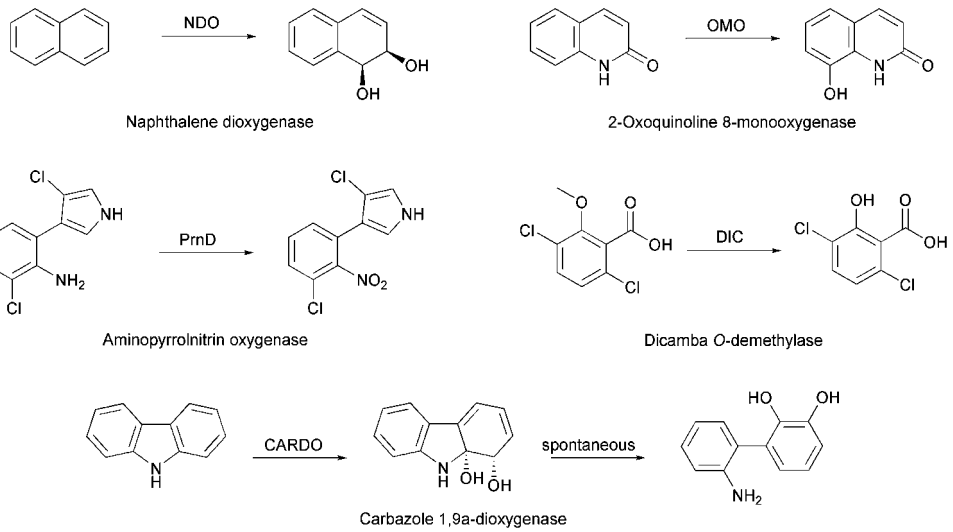

Fig. 7 Some examples of reactions catalyzed by different mononuclear non-heme iron Rieske oxygenases.

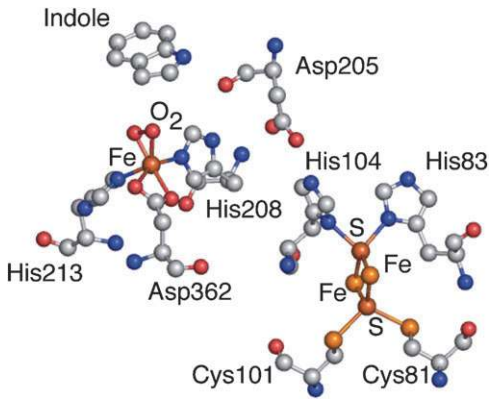

Fig. 8 Dioxygen bound side-on to the metal center in naphthalene dioxygenase (NDO) with bound substrate analogue indole (1O7N.pdb). The [2Fe–2S] Rieske cluster and a conserved aspartate are also shown.

(NDO).[52,53] Several three-dimensional structures including a dioxygen adduct of an enzyme–substrate analogue complex have been reported. The structural features of the latter complex are depicted in Fig. 8.

The structures show that the aspartate residue of the structural motif is bound in a bidentate fashion to the metal center, in a variation of the 2-His-1-carboxylate facial triad. Dioxygen is bound side-on to the iron and, based on the O–O bond length of 1.4 Å, is reduced to the peroxide level.[52] Interestingly, the structure of NDO–Fe(II)–indole–NO shows an end-on bound nitric oxide.[54] Nitric oxide is often used as an unreactive analogue of dioxygen, but these results show that one has to be cautious in correlating NO binding data to dioxygen binding directly.[54] In the last two years crystallographic data of several other Rieske oxygenases have been reported. The structures of biphenyl dioxygenase,[55] nitrobenzene dioxygenase,[56] cumene dioxygenase,[57] carbazole-1-9a-dioxygenase,[58] and 2-oxoquinoline 8-monooxygenase[49] show a high structural similarity to naphthalene dioxygenase with all key features present. An interesting variation amongst the reported structures is the binding mode of the aspartate of the 2-His-1-carboxylate structural motif. Whereas a bidentate aspartate was observed in NDO, monodentate binding is found in the enzyme-substrate complex of biphenyl dioxygenase[55] and the as-isolated states of cumene dioxygenase[57] and nitrobenzene dioxygenase.[56] In the latter case, the binding mode of the aspartate changes to bidentate upon substrate binding. The crystal structures of two enzymes capable of the oxidation of large polycyclic aromatic hydrocarbons with up to five aromatic rings have also become available. The broad substrate specificity of both ring-hydroxylating dioxygenase from *Sphingomonas* CHY-1[59] and biphenyl 2,3-dioxygenase from *Sphingobium yanoikuyae* B1[44] mainly originates from a larger entrance to the active site and a substantially larger hydrophobic substrate binding pocket. The first structure of the oxygenase ferredoxin electron transfer complex of a Rieske oxygenase system has also been reported.[60] In the binary oxygenase–ferrodoxin complex of carbazole 1,9a-dioxygenase three ferrodoxins bind to the trimeric oxygenase molecule, thus forming a trimer of heterodimers. Significant conformational changes result in specific binding interactions which properly align the Rieske clusters of the ferrodoxin and terminal oxygenase components for electron transfer (approximate distance of 12–13 Å).[60]

The general mechanism of dioxygen activation is believed to be the same for all Rieske oxygenases, but subtle differences have been noted (*vide infra*) (Fig. 9).[15] The binding of dioxygen to the metal is enhanced upon substrate binding through the conversion to a five-coordinate metal center.[3] The reactivity of the ferrous center is, furthermore, controlled allosterically by the redox state of the Rieske cofactor. Reduction of the cluster leads to conformational changes at the active site, opening up a pathway for dioxygen.[49] A side-on iron–(hydro)peroxide complex is formed upon binding of dioxygen and electron transfer from the Rieske cluster,[7,15] consistent with the crystallographically characterized dioxygen adduct.[52] From this point on, different mechanisms for the actual oxygen insertion steps have been proposed. A key difference is the fate of the iron(III)–(hydro)peroxide intermediate, which can either act as the reactive species itself and

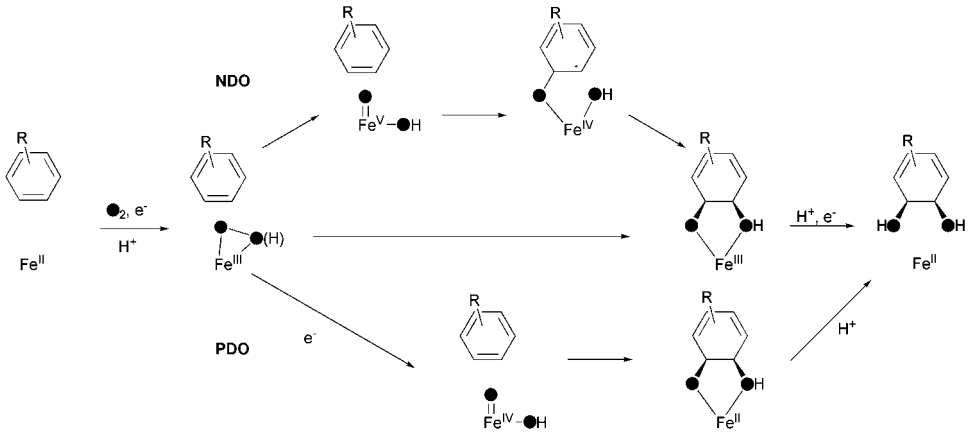

Fig. 9 Different possible pathways in the *cis*-dihydroxylation of naphthalene (top, NDO) and phthalate (bottom, PDO). The different timing of electron transfers to the mononuclear center leads to different high-valent iron–oxo intermediates.[66] The direct attack of the substrate by the hydroperoxo species has also been included.

directly attack a substrate or, alternatively, first undergo O–O bond cleavage to yield an HO–Fe(v)═O intermediate. Some authors prefer the former, direct attack of substrate by the side-on (hydro)peroxide species, since there is no need then to invoke any higher oxidation states of iron.[15] Computational studies also implicate a concerted step, where the O–O bond is cleaved concomitantly with the formation of an epoxide. This epoxide intermediate would subsequently evolve toward an arene cation, and finally to the *cis*-diol. A high activation barrier was found for the mechanism involving O–O bond cleavage prior to attack of the substrate.[61,62]

The latter option of O–O cleavage prior to substrate oxidation would give rise to either cationic or radical intermediates. This pathway has been favored by others based on isotope labeling experiments which show some oxygen exchange of the active species with labeled water in the enzymes.[7] Isotope labeling studies with a biomimetic family of non-heme iron catalysts that carry out *cis*-dihydroxylation reactions also show significant oxygen exchange, which points at O–O bond cleavage and formation of a high-valent iron–oxo intermediate.[63]

In a very recent contribution, single turnover studies of the monooxygenase reaction of NDO with the diagnostic bicyclic probes norcarane and bicyclohexane have unequivocally shown that at least these *mono*oxygenation reactions occur *via* radical intermediates (Fig. 9, top), since radical rearrangement products of each probe are observed in substantial amounts.[64] This supports O–O bond cleavage prior to substrate attack and the formation of a high-valent Fe(v) oxidizing species.[64] The isolation and characterization of both iron(IV)[24] and, very recently, iron(v)–oxo species[26] in model complexes has given further support for the accessibility of such high-valent species in a non-heme iron environment (*vide infra*).

Single turnover experiments have also shown that the chemical reaction can be achieved without the reductase and/or ferredoxin components.[64–66] Subtle differences are, however, observed between different dioxygenases in these single turnover experiments. The reaction of reduced NDO or benzoate dioxygenase (BZDO) with dioxygen resulted in the formation of one equivalent of product per Rieske center oxidized and the mononuclear iron center ends up in the ferric oxidation state.[65] In contrast, reaction of reduced phthalate dioxygenase (PDO) with dioxygen gave only half an equivalent of product per Rieske center oxidized and a resulting ferrous metal center,[66] pointing at different oxidation mechanisms for these substrates. Based on these observations, it has been proposed that a difference in timing of the electron transfers to the mononuclear center leads to different high-valent iron–oxo intermediates, *i.e.* Fe(v) for NDO and BDZO and Fe(IV) for PDO (Fig. 9). The formation of the more strongly oxidizing Fe(v) species in the former systems would then in turn explain the wide range of oxygenation reactions catalyzed by NDO compared to the tighter substrate selectivity of PDO.[66]

The chemo-, regio- and stereoselectivities of the specific reactions catalyzed by the different Rieske oxygenases seem determined solely by the specific orientation of the substrate in the binding pocket of the enzyme. Interactions between active site residues and the substrate through, for instance, hydrogen bonds determine this orientation.[15,67] In the substrate bound structure of carbazole 1,9a-dioxygenase, for instance, a hydrogen bond from the imino nitrogen of the substrate carbazole to the carbonyl oxygen of Gly178 is critical for the proper orientation of the substrate.[58]

3.3 α-Ketoglutarate-dependent enzymes

The largest subfamily of non-heme iron enzymes with the 2-His-1-carboxylate facial triad couples the oxidative transformation of substrates to the oxidative decarboxylation of the cofactor α-ketoglutarate (α-KG) to carbon dioxide and succinate.[7] This subfamily is not only the largest, but also catalyzes the most diverse set of oxidative transformations. Reactions include hydroxylation, desaturation, ring closure, ring expansion, epimerization and many more. As a result, these enzymes are involved in processes as diverse as the synthesis of antibiotics, DNA repair, oxygen sensing, and transcription regulation. The subfamily constitutes probably the most versatile group of oxidizing biological catalysts identified to date.[68] Many of these transformations are at the moment

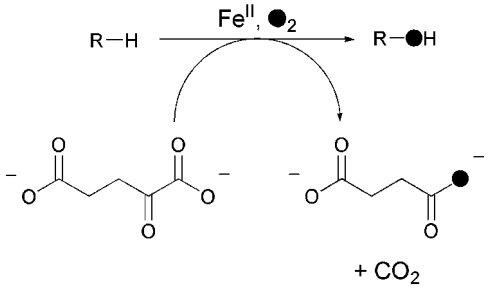

Fig. 10 General hydroxylation reaction catalyzed by many of the α-KG-dependent oxygenases.

beyond the scope of synthetic organic chemists and are therefore of special chemical interest.[68] Several different reviews have been published recently that are specifically devoted to this subfamily of enzymes.[68–72] A recent comprehensive sampling of the reactivities of the currently known α-ketoglutarate-dependent enzymes is available as well.[71] Here, we will therefore only address some general features and typical examples. Hydroxylation, for instance, is the most common reaction observed and its general scheme is shown in Fig. 10.

Two types of hydroxylation reactions have recently received increased attention out of medical interest. Damage of RNA and DNA by nucleotide alkylation, for instance, results in lesions that are both cytotoxic and mutagenic.[73] Several α-KG-dependent oxygenases have been shown to repair these alkylated DNA and RNA bases. Escherichia coli AlkB and the homologous human enzyme ABH3 fix the lesion by hydroxylating the alkyl group, after which spontaneous deformylation yields the unmodified base (Fig. 11A).[73–75]

Other, related demethylation reactions catalyzed by α-KG-dependent enzymes, such as histone demethylation, have been reported recently as well.[76,77] The hydroxylation of specific residues of protein side chains and more specifically in oxygen sensing in the cell has also attracted recent interest. Hypoxia-inducible factor (HIF) is responsible for mediating the mammalian response to low oxygen tension (hypoxia). α-KG-dependent HIF hydroxylases[78] have been implicated in this hypoxic response and are therefore interesting targets for the development of new therapies for the different diseases associated with this system.[79] Other functions of the α-KG-dependent oxygenases include the biosynthesis of antibiotics and plant products, lipid metabolism and biodegradation.[69] Some selected examples are shown in Fig. 11.

Crystallographic data on many different α-KG-dependent oxygenases have been reported over the last 10 years and the more than 50 available structures[71] now provide a wealth of structural information. These crystallographic studies of the α-ketoglutarate-dependent enzymes and related enzymes have been reviewed recently.[68] The ternary TauD–Fe(II)–α-KG–substrate complex, for instance, shows a five-coordinate metal center with the α-KG cofactor bound in a bidentate way (Fig. 12). The cofactor is further held in place by additional interactions of the C5-carboxylate with conserved residues. The primary substrate is not bound directly to the metal center, but is found close to the open coordination site, which is believed to be the site of dioxygen binding. TauD catalyzes the hydroxylation of taurine (2-aminoethane-1-sulfonic acid), which leads eventually to sulfite elimination from the product.[17]

The large body of crystallographic data together with spectroscopic studies on especially TauD[17] and CAS[80] has led to the proposal of a common, conserved mechanism for the α-KG-dependent oxygenases (Fig. 12).[7,17,68,69]

In this general mechanism, an ordered sequential binding of first α-KG, then substrate and finally dioxygen is assumed. Structural and spectroscopic studies show an octahedral iron(II) metal center in the holo enzymes with the facial triad and three water molecules completing the coordination sphere (A).[71] Subsequently, the α-ketoglutarate binds in a bidentate fashion by displacing two water molecules and the metal

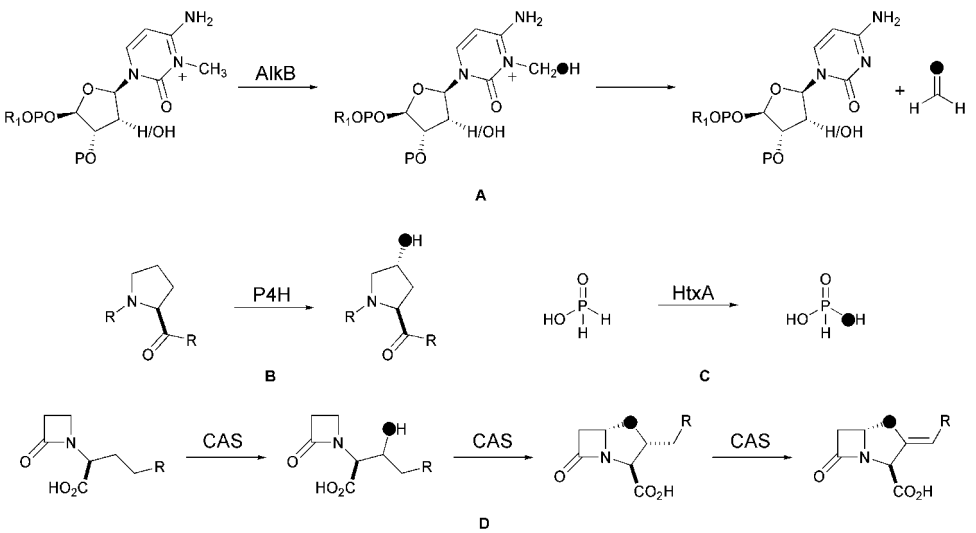

Fig. 11 Some selected examples of reactions catalyzed by α-KG-dependent oxygenases. (A) Nucleobase demethylation by DNA/RNA repair enzyme AlkB; (B) Stereospecific proline hydroxylation by proline 4-hydroxylase (P4H); (C) Hypophosphite hydroxylation by hypophosphite/α-KG dioxygenase HtxA; (D) Hydroxylation, ring closure and desaturation reactions in the synthesis of clavulanic acid by clavaminate synthase CAS.

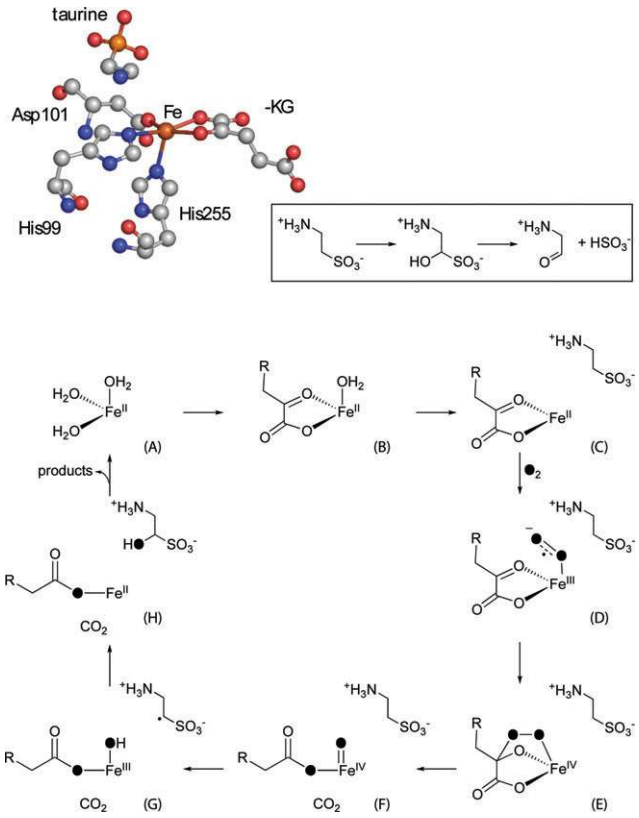

Fig. 12 Top: Active site of the ternary TauD–Fe(II)–α-KG–taurine complex (1OS7.pdb).[81] Bottom: Consensus mechanism for α-KG-dependent hydroxylases, exemplified for TauD (adapted from ref. 17).

center remains six-coordinated (B). The bidentate binding of the α-keto acid gives rise to a very characteristic set of MLCT transitions in the visible region (around 500 nm).[82] The native substrate then binds in the proximity of (but not directly to) the metal ion and upon substrate-binding the remaining water ligand is lost and, in almost all cases, the coordination around the ferrous ion changes to five-coordinate square-pyramidal (C). This change in coordination number has been crystallographically established in, among others, the structures of TauD,[83] DAOCS,[84] and Alkylsulfatase (AtsK),[85] which were crystallized in the presence of α-ketoglutarate and their respective native substrates. The displacement of the last water molecule is thought to be essential for catalysis and poises the metal for reaction with dioxygen. The greatly enhanced reactivity of the metal center towards dioxygen *after* substrate binding effectively favors the generation of the (potentially damaging) reactive intermediates only in the presence of the target substrate and in this way protects the enzyme from inactivation by self-hydroxylation reactions. Such self-hydroxylation of nearby amino acid residues in the absence of substrate has in fact been observed for a number of non-heme iron enzymes, including some α-ketoglutarate-dependent enzymes.[86] It has been proposed that this self-modification serves to protect the enzyme from chemical damage in the absence of substrate, but the physiological function and significance is currently not completely clear and subject of discussion.[71,86]

In the presence of substrate, the binding of dioxygen results in the formation of an adduct with significant Fe(III)-superoxide radical anion character (D).[87] Nucleophilic attack of the carbonyl carbon atom by this species would then result in a cyclic ferryl bridged-peroxo species (E). In the next step, decarboxylation and O–O bond cleavage yield succinate, carbon dioxide and a high-valent Fe(IV)=O species (F), which is the intermediate responsible for the substrate oxidation leading to hydroxylation or a related two-electron oxidation.[17] This ferryl intermediate was first observed experimentally for TauD by rapid freeze-quench Mössbauer,[18] and its presence confirmed by EXAFS,[20] and resonance Raman studies.[19] These spectroscopic studies revealed species with a high-spin ($S = 2$) configuration,[18] a characteristic isotope-sensitive iron–oxo vibration in the 800 cm^{-1} region,[19] and a short Fe–O interaction of 1.62 Å.[20] Most importantly, these studies provided the first direct evidence of the involvement of an iron(IV) intermediate in reactions catalyzed by mononuclear non-heme iron enzymes.

From this point on the chemistry of each enzyme diverges and different subsequent steps result in the rich variety of oxidative transformations that this subgroup catalyzes. It has been suggested that the chemistry that follows after the generation of the pivotal ferryl–oxo species results mainly from the structural characteristics of the specific substrate. In all the different enzymes of the subgroup, the Fe(IV)=O intermediate is generated in the same ligand environment and should, therefore, be capable of facilitating all different kinds of observed reactivity.[71] In the TauD example, abstraction of a hydrogen atom (G), followed by recombination of the coordinated hydroxyl radical with the substrate radical yields the hydroxylated product (H). The observation of a large substrate deuterium kinetic isotope effect on the decay of the ferryl species identified it as the hydrogen-abstracting intermediate.[88] A C–H cleaving high-spin Fe(IV) complex with strikingly similar spectroscopic and kinetic characteristics has also been detected in prolyl-4-hydroxylase (P4H), which is only distantly related to TauD.[21] These results support the view of a conserved mechanism within the α-ketoglutarate hydroxylases. In line with this, Purpero and Moran illustrated that all other currently known reactivities can be envisaged to proceed along either such one-electron hydrogen atom abstraction pathways (as in TauD), or alternatively through two-electron or hydride-abstraction pathways.[71]

The α-KG-dependent non-heme iron enzymes (4-hydroxyphenyl)pyruvate dioxygenase (HppD)[89] and (4-hydroxy)-mandelate synthase (HmaS)[90] form an interesting pair in the sense that they use the same substrate, (4-hydroxyphenyl)-pyruvate which itself has an α-keto acid moiety (Fig. 13). As a result both atoms of dioxygen are incorporated into the product, similar to the extradiol cleaving dioxygenases. HppD

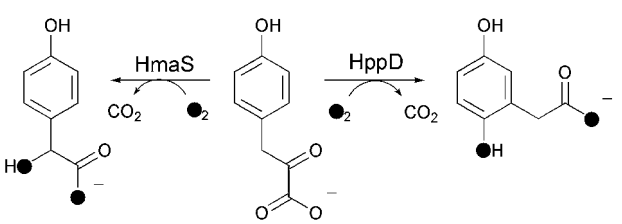

Fig. 13 Oxidative transformations of (4-hydroxyphenyl)pyruvate catalyzed by HmaS and HppD.

yields the aromatic hydroxylated product homogentisate using an electrophilic attack mechanism followed by an NIH shift, whereas HmaS generates the benzylic hydroxylated product (*S*)-(4-hydroxy)mandelate *via* a hydrogen abstraction mechanism.[91] The two enzymes generate the same reactive Fe(IV)=O intermediate, but are able to steer the reaction into two different directions. The decisive factor was found to be the exact orientation of the substrate in the enzyme binding pocket.[91]

Recently, a group of non-heme iron enzymes with quite a different reactivity has been discovered.[92] Rather than hydroxylation, these enzymes catalyze the halogenation of aliphatic C–H bonds and require Fe(II), α-KG, dioxygen and chloride for activity. The enzymes SyrB2[93] and CmaB[94] are involved in the biosynthesis of the phytotoxin syringomycin E and the phytotoxin precursor coronamic acid, respectively. Syr2B catalyzes the chlorination of a threonine methyl group, whereas CmaB catalyzes the γ-halogenation of L-*allo*-isoleucine as part of a cryptic biological strategy for cyclopropyl ring formation (Fig. 14). The non-heme iron halogenation catalysts are not limited to the two enzymes mentioned here, as bioinformatic analysis has provided leads to additional members of this interesting new group.[92] CytC3, for example, chlorinates L-aminobutyrate to γ-chloroaminobutyrate[95] or, if allowed to proceed through multiple turnovers, even to γ,γ-dichloroaminobutyrate. The free dichloroamino acid is a known antibacterial natural product.[92] Multiple chlorinations were also observed for the Syr2B homologues BarB1 and BarB2, which catalyze the tandem trichlorination of L-leucine as part of the biosynthesis of the marine natural product barbamide[96] (Fig. 14).

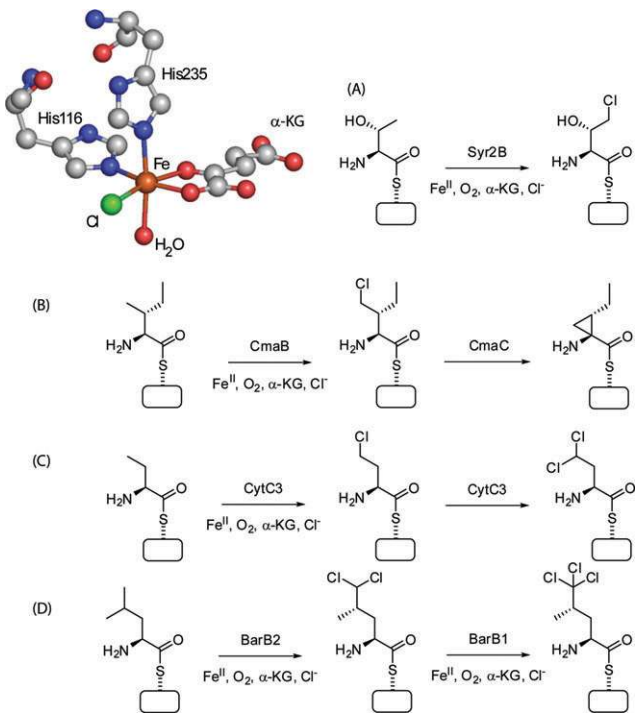

Fig. 14 An unprecedented iron scaffold found at the active site of Syr2B. (A) The halogenation reactions catalyzed by Syr2B, and (B) CmaB, (C) CytC3, and (D) BarB1 and BarB2.

The crystal structure of the Syr2B–Fe(II)–α-KG complex was solved very recently. As a surprising result, it presented the first α-KG-dependent non-heme iron enzyme *not* coordinated by the 2-His-1-carboxylate facial triad.[97] Instead, the metal is coordinated by α-KG, a chloride anion and only two endogenous ligands. *i.e.* two histidines (Fig. 14). An alanine replaces the aspartate of the facial triad. The mechanism of halogenation is thought to be similar to the common hydroxylation mechanism with chloride abstraction instead of hydroxyl abstraction by the carbon radical in the final step.[97] Mössbauer and absorption spectroscopic studies on the chlorination reaction by CytC3 identified two rapidly interconverting high-spin Fe(IV) intermediates and a marked substrate deuterium kinetic isotope effect on the decay of these ferryl species implicated them as the hydrogen atom-abstracting complex.[22] The presence of two rather than one Fe(IV) intermediate contrasts with the observations made for TauD and P4H. The authors speculate that the two intermediates might be two rapidly-converting conformers of a Cl–Fe(IV)-oxo complex.[72] A very recent spectroscopic study of CytC3 in the analogous reaction with bromide provided further evidence for direct coordination of a halogen to the high-valent iron and the assignment of these high-spin iron(IV) intermediates as a Br–Fe(IV)–oxo species.[98] Freeze-quench Fe K-edge X-ray absorption spectroscopy revealed short Fe–O and Fe–Br interactions of 1.62 and 2.43 Å, respectively.[98] These results further emphasize the similarities between the α-KG-dependent halogenases and hydroxylases.

3.4 Pterin-dependent hydroxylases

The small family of aromatic amino acid hydroxylases (AAAH) requires the cofactor tetrahydrobiopterin (BH_4) for activity.[1,7] Its members phenylalanine hydroxylase (PheH), tyrosine hydroxylase (TyrH), and tryptophan hydroxylase (TrpH) are essential for mammalian physiology. In contrast to TyrH and TrpH, which are only found in eukaryotes, PheH has also been identified in prokaryotes.[7] The enzymes catalyze the regiospecific monohydroxylation of their namesake amino acids with concomitant oxidation of the pterin cofactor (Fig. 15). TyrH catalyzes the initial step in the catecholamine neurotransmitters biosynthesis, PheH catabolises excess phenylalanine and TrpH is involved in the synthesis of the neurotransmitter serotonin.

This group of enzymes has received considerable attention because of their implication in some neurological and physiological diseases. Several different reviews are available that comprehensively discuss the current state of knowledge of this sub-family.[1,7,18,99,100] The three enzymes show significant sequence and structural similarity. Crystal structures, which have been reported for all three enzymes,[101–104] clearly illustrate the structural homology especially at the active site. They feature a mononuclear non-heme iron active site, coordinated by the 2-His-1-carboxylate facial triad and three water molecules. It has been noted that in bacterial PheH (cPheH) the equatorial glutamate ligand acts as a bidentate ligand rather than the monodentate binding mode observed in human PheH.[105] The bacterial PheH structure was, however, solved with the catalytically inactive Fe(III) form of the enzyme.[105]

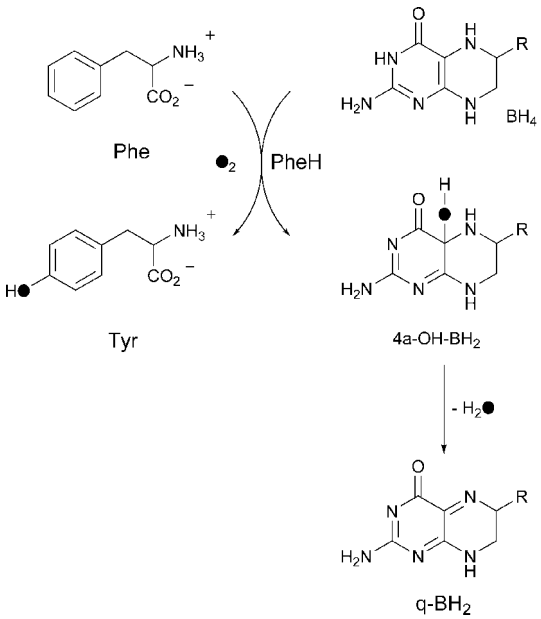

Fig. 15 Hydroxylation of phenylalanine (Phe) to tyrosine (Tyr) catalyzed by phenylalanine hydroxylase (PheH).

Interestingly, large conformational changes upon pterin and substrate binding are observed at the active site in the crystal structure of PheH–Fe(II)–BH_4–tha (tha, 3-(2-thienyl)-l-alanine, a substrate analogue).[106] In contrast to the other subfamilies, in this case neither the substrate nor the cofactor binds directly to the metal center. The monodentate glutamate becomes bidentate, water molecules are lost and the pterin cofactor is displaced towards the iron (Fig. 16). All these changes facilitate the binding of dioxygen at the active site. EPR and UV-Vis studies on nitric oxide adducts of bacterial PheH in the presence of substrate and cofactor suggest that, upon binding, dioxygen replaces the last remaining water molecule to afford a five-coordinate iron, rather than the formation of a six-coordinated metal center through coordination to an open site (Fig. 16A).[107]

The plethora of spectroscopic and structural data has led to a consensus about the possible mechanism, although up till recently none of the (reactive) intermediates had been directly observed.[1,7,108] The study of kinetic isotope effects on the aromatic hydroxylation reactions provided evidence that all three enzymes operate *via* the same mechanism, albeit with different rate-limiting steps.[109] The proposed mechanism is depicted in Fig. 16, exemplified for PheH. First, a (putative) pterinperoxo–iron(II) species is formed (B), which cleaves heterolytically to yield a reactive iron(IV)–oxo intermediate (C). Very recently, direct spectroscopic evidence for such a high-spin Fe(IV) intermediate has been reported for TyrH.[110] The complex TyrH–Fe(II)–6-MePH4–Tyr was exposed to dioxygen and quenched by rapid-freeze (6-MePH4, 6-methyltetrahydropterin). Mössbauer spectroscopic measurements revealed an intermediate with features similar to the high-spin Fe(IV) species observed for the α-ketoglutarate-dependent enzymes. Kinetic experiments furthermore revealed this species, presumably the postulated Fe(IV)–oxo (C), to be the hydroxylating intermediate. A study on benzylic hydroxylation

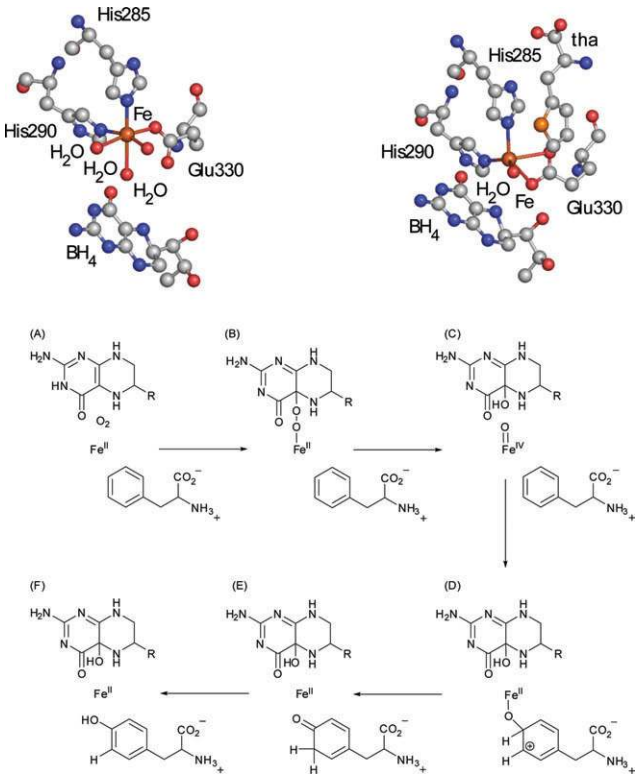

Fig. 16 Top: Structural changes upon substrate binding to the active site of phenylalanine hydroxylase: the binary PheH–Fe(II)–BH_4 complex (1J8U.pdb) (left) and the ternary PheH–Fe(II)–BH_4–tha complex (1KW0.pdb) (right). Bottom: Proposed reaction mechanism for the AAAHs, exemplified for PheH (adapted from Fitzpatrick *et al.*[109]).

by the three AAAHs gave similar intrinsic kinetic isotope effects, suggesting that the reactivities of the hydroxylating intermediates are very similar among the three enzymes.[111]

Electrophilic attack of the substrate then results in a cationic intermediate (D). Kinetic isotope effects have been determined for all three enzymes. In the case of TrpH an inverse isotope effect was found, consistent with the hydroxylation being the rate limiting step.[112] For TyrH and PheH the obtained results for the wild-type enzymes were less straightforward, but in both cases isotope effects could be unmasked by the use of mutant enzymes, which allowed for the partitioning of intermediates *via* branched pathways.[113] This uncoupling resulted in the observation of the expected isotope effects for both TyrH[113] and PheH.[109] An NIH-shift and subsequent tautomerisation ultimately result in product formation (E, F).

3.5 Miscellaneous

This category is a diverse collection of enzymes that do not fit into the previous four classes with respect to their specific requirements for catalysis. It is a 'catch-all' category and some recent discoveries have been included. These newly discovered metalloenzymes catalyze unprecedented chemical reactions and offer a glimpse of the systems and their chemistry that still are to be discovered.

The enzyme *sulfur oxygenase reductase* (SOR), for instance, catalyzes a distinctive oxygen-dependent sulfur disproportionation reaction with sulfite, thiosulfate, and hydrogen sulfide

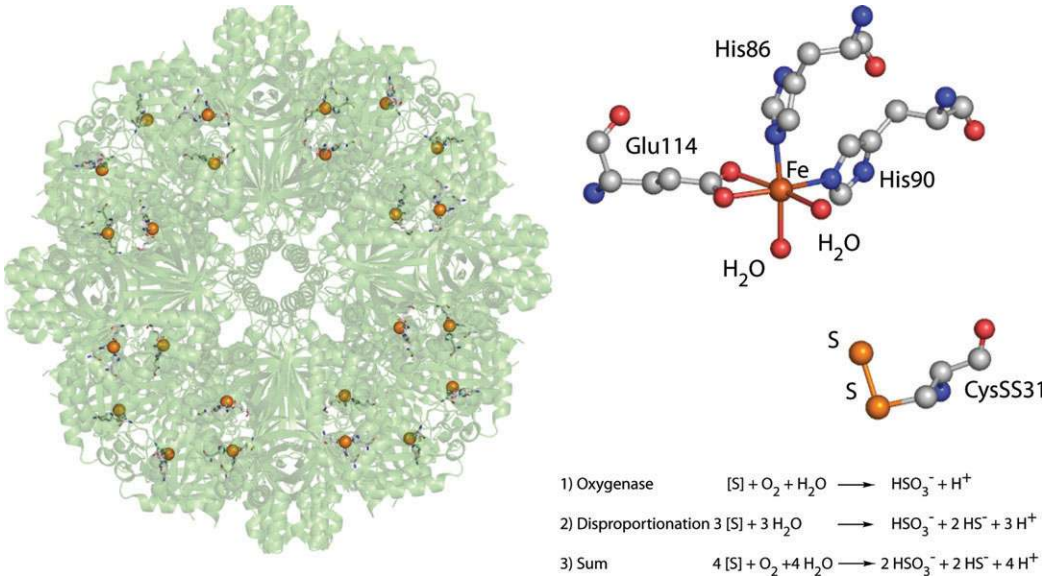

Fig. 17 Left: Sulfur oxygenase reductase (SOR) is a complex, self-compartmentalizing metalloenzyme that consists of 24 subunits and forms a hollow sphere (active sites highlighted). Right: The active site of SOR shows a bidentate glutamate residue and a cysteine persulfide as the substrate binding site (2CB2.pdb).

as the products without the need of external cofactors or electron carriers (Fig. 17, right).[114] Oxidized and reduced products form in a 1 : 1 stoichiometry in the catalytic reaction.

SOR is one of the few systems known to oxidize elemental sulfur, an essential reaction for ecosystems that use sulfur as the major energy source. The *Acidianus ambivalens* SOR is a complex, self-compartmentalizing metalloenzyme that consists of 24 subunits and forms a hollow sphere (Fig. 17, left).[114] A mononuclear non-heme iron site and a cysteine persulfide (CysSS31) were found to be important for catalysis. The latter is the probable covalent binding site for *linear*, rather than regular α-S_8 elemental sulfur substrate and has the terminal sulfane oriented to the iron site. Two other cysteine residues are found in known SOR sequences, but site-directed mutagenesis studies have shown that these residues optimize reaction conditions, but are not essential for catalysis.[115,116] Mutations of either one of the iron binding residues and the cysteine persulfide resulted in complete inactivation of the enzyme.[116]

As previously observed for some of the Rieske dioxygenases, the glutamate of the 2-His-1-carboxylate structural motif coordinated to the iron center is bound as a bidentate to the metal. Two water molecules complete the distorted octahedral coordination sphere. The mononuclear non-heme iron site has an unusually low reduction potential (−268 mV), which may result from hydrogen bonding interactions around the metal site. Since no other redox-active site was found in SOR, the rather complicated sulfur disproportionation chemistry has to take place at the iron active site.

Fosfomycin, or (1*R*,2*S*)-1,2-epoxypropylphosphonic acid, is a clinically useful antibiotic and is for instance used in the treatment of lower urinary tract infections. It is also effective against methicillin-resistant and vancomycin-resistant strains of *Staphylococcus aureus*.[117] The last step in the biosynthesis of fosfomycin in *Streptomyces wedmorensis* is the dehydrogenation of (*S*)-2-hydroxypropylphosphonic acid (Hpp) by Hpp epoxidase (HppE) (Fig. 18). HppE was recognized as a non-heme iron enzyme belonging to the class featuring the facial triad.[118–120] This reaction is unique in biology since the

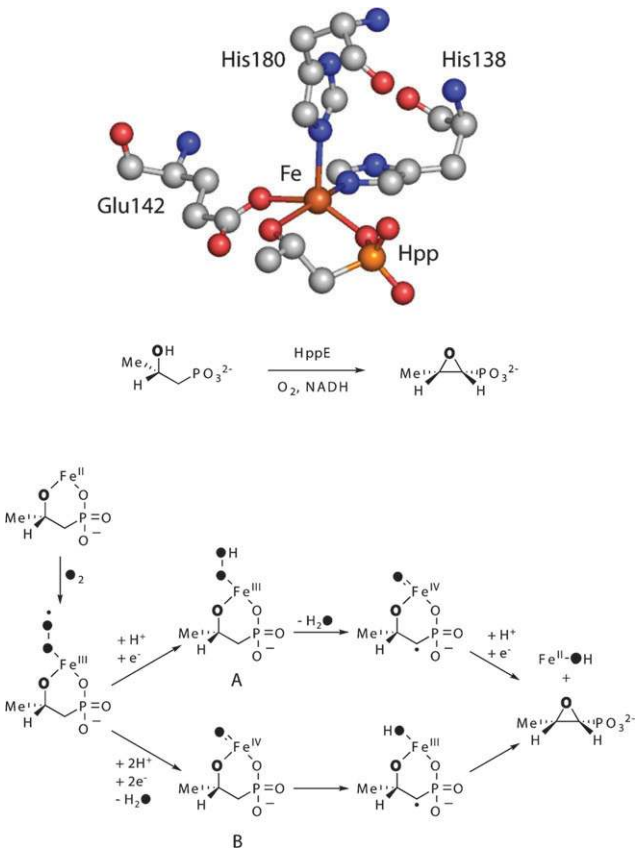

Fig. 18 The enzyme-substrate complex of HppE with the substrate bound in a bidentate fashion (1ZZ8.pdb) and two possible mechanisms, going through either an iron(III)–hydroperoxide (A) or iron(IV)–oxo species (B).

epoxidation reaction is an oxidative cyclization with retention of the substrate hydroxyl oxygen atom, *i.e.* a dehydrogenation of a secondary alcohol.[119] Usually, in epoxidations such as those catalyzed by cytochrome P450, the incorporated oxygen atom is derived from dioxygen.[6] A catalytic turnover of HppE consumes a stoichiometric amount of NADH with molecular oxygen as the oxidant,[119] similar to the previously described Rieske dioxygenases. The putative reductase, however, remains to be identified. Recently, crystal structures of the native enzyme and the enzyme-substrate complex became available.[117] Two different binding modes are observed in the crystal structure, a monodentate and bidendate one. In the monodentate binding mode the substrate is bound through an oxygen atom of the phosphonic acid moiety displacing one water molecule. In the bidentate binding mode the substrate replaces two of the water molecules and binds to the metal through the 2-hydroxyl oxygen and the phosphonic acid oxygen. These two observed binding modes thus suggest a two-step binding process before catalysis. Conformational changes upon substrate binding create an extensive hydrogen-bonding network between the substrate, bound water molecules and the enzyme.[117] The formation of a five-coordinate iron center upon bidentate binding of the substrate would again activate the metal center for dioxygen activation. The stereo- and regiospecific hydrogen abstraction step is then catalyzed by either an iron(III)–hydroperoxide (Fig. 18, path A) or iron(IV)–oxo (path B) species to give a substrate radical intermediate. Cyclization of the radical yields the final two-electron oxidized product. The regiospecificity of the hydrogen abstraction step and consequently the stereochemical outcome of the reaction appears to be determined by the relative orientation of the C–H bonds of the bound substrate.[117,118] This is further supported by the fact that Hppe was found not to be selective with regard to substrate recognition as it accepts both (*R*)- and (*S*)-Hpp, but it does stereospecifically convert each enantiomer into a unique product.[118]

An alternative mechanism has been proposed based on the observation that a Zn(II)-reconstituted HppE in the presence of flavin mononucleotide is active as well.[121] The crystal structures of Zn(II)-reconstituted HppE and its fosfomycin complex were reported. The activity with the redox inert Zn(II) metal center suggested the metal to merely serve as a Lewis acid and a new 'nucleophilic displacement-hydride transfer' mechanism was proposed.[121] However, a re-examination of these results showed that Zn(II)-reconstituted HppE is actually catalytically inactive and reconfirmed that iron is required for HppE catalysis.[120]

Interestingly, next to the unusual physiological reaction of HppE, the enzyme can also catalyze a more typical oxygenase reaction. Upon exposure to air HppE catalyzes the self-hydroxylation of an active site tyrosine residue resulting in a green chromophore identified as a bidentate iron(III)–catecholato complex.[122] This oxygenase activity implies the involvement of a putative high-valent iron–oxo or iron–hydroperoxide intermediate. A significant observation, since the same reactive intermediate is proposed in the mechanism for fosfomycin biosynthesis.[117,120]

The enzyme HppE shows similarities with the microbial enzyme *isopenicillin N synthase* (IPNS). IPNS is a non-heme iron enzyme that catalyzes the double oxidative ring closure of the tripeptide δ-(L-α-aminoadipoyl)-L-cysteinyl-D-valine (acv) to form the bicyclic β-lactam isopenicillin N, the biosynthetic precursor to all penicillins and cephalosporins (Fig. 19).[7,123]

IPNS shows a high sequence homology to the α-ketoglutarate-dependent enzymes, but does not require α-ketoglutarate as cofactor and it does not incorporate oxygen into the product.[7] In the case of IPNS all four electrons required for the reduction of dioxygen to water are provided by the substrate. Crystal structures are available for different stages of the reaction,[124–126] such as the ternary IPNS–Fe(II)–acv–NO complex.[126] Nitric oxide (NO) is often used as an unreactive O_2-surrogate to get more insight into the interaction of dioxygen with the metal. Based on this information and comprehensive studies with substrate analogues by Baldwin and co-workers,[7,123,127,128] a mechanism has been proposed. The closure of the β-lactam precedes the formation of the thiazolidine ring and an iron(III)–superoxide species has been invoked as the oxidizing species in this particular step. Spectroscopic and computational studies by Solomon and co-workers have shown, that the thiolate-bound substrate stabilizes the formation of such an end-on superoxide, which in turn has the proper electronic configuration and orbital orientation for hydrogen abstraction.[27] The hydrogen abstraction step then results in the first oxidative ring closure product (β-lactam) and in the formation of a high-valent iron(IV)–oxo species. The latter species mediates the second oxidative ring closure, *i.e.* the thiazolidine ring formation.

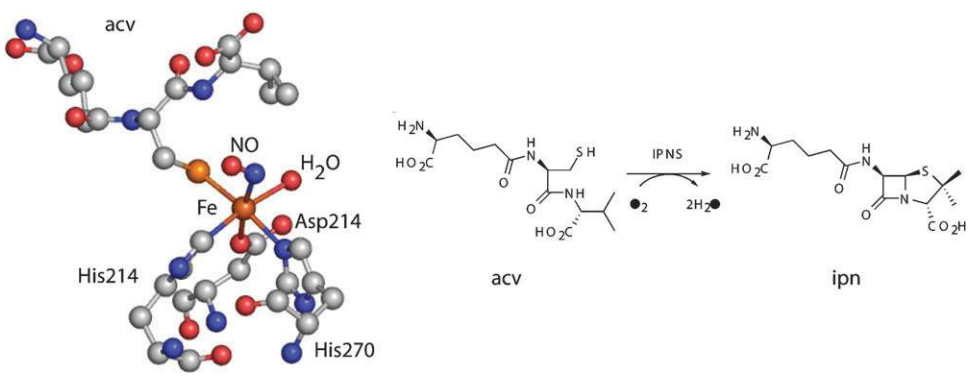

Fig. 19 Active site of the ternary IPNS–Fe(II)–acv–NO complex and the oxidative double ring closure catalyzed by IPNS.

The enzymology of IPNS and other enzymes involved in the biosynthesis of β-lactam derived compounds has been recently reviewed.[123]

The enzyme *1-aminocyclopropane-1-carboxylic acid oxidase* (ACCO) also shows a high sequence homology to the α-ketoglutarate-dependent enzymes, but like IPNS does not require α-ketoglutarate as cofactor.[7] ACCO is an enzyme that produces the plant hormone ethylene, which regulates many aspects of plant growth and development, such as fruit ripening. This makes ACCO an attractive target for regulation of this agriculturally important process.[129] The enzyme couples the reduction of dioxygen to two water molecules to the two-electron oxidation of the unusual amino acid 1-aminocyclopropane-1-carboxylic acid (acc) to give ethylene, CO_2 and HCN (Fig. 20).[7] Due to the lack of available structural information and the inherent complexity of the system, the mechanism of ACCO is not yet fully understood.[130,131]

Continuous turnover requires both the presence of ascorbate and bicarbonate. The latter acts as an activator, *i.e.* stimulates catalysis independent of its redox properties, and increases the k_{cat} and protects ACCO from oxidative deactivation.[132] It is known that, in the presence of bicarbonate, the substrate acc binds in a bidentate fashion through its amino and carboxylate groups.[3,133] This enzyme-substrate complex is, however, insufficiently reactive to effect acc oxidation and ascorbate must bind to the enzyme as well to convert the Fe(II) site from six- to five-coordinate and activate it for dioxygen binding.[133] Therefore, in addition to its traditional role as two-electron reducing agent,[132] ascorbate may also act as an activator by binding at a (remote) specific effector site and thus facilitating the formation of the ternary enzyme–substrate–dioxygen complex.[134] The ternary ACCO–Fe(II)–acc–NO complex has indeed been observed by ENDOR spectroscopy.[135] The ENDOR studies furthermore suggested that the orientation of substrate binding is dictated by the enzyme, which in turn determined the orientation of bound NO and, by analogy, O_2.

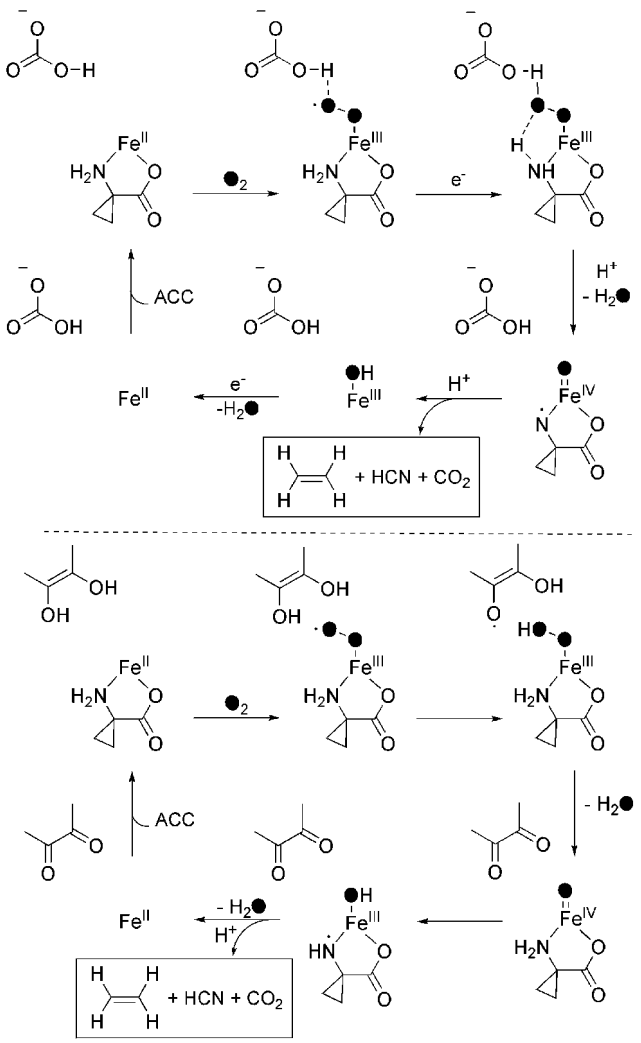

Fig. 20 Mechanisms for ACCO catalysis proposed by Rocklin *et al.*[132] (top) and Thrower *et al.* (bottom).[129]

The subsequent source and sequence of electron donation to dioxygen and the mode of dioxygen activation are longstanding questions in the study of the mechanism of ACCO, since both substrate and ascorbate can function as a single electron donor. In any case, after one-electron transfer from ascorbate, the formation of an iron–oxo species, be it Fe(III)–OOH or, after O–O fission, Fe(IV)=O is proposed. Bicarbonate is proposed to be involved in the generation of the reactive species by a specific protonation step.[132] Thrower *et al.* found in a kinetic study of the reaction of ACCO with different cyclic and acyclic substrate analogues that k_{cat} was almost indifferent to substrate structure.[129] This and other observations pointed to a rate-determining step that precedes substrate activation and a high-valent iron(IV)–oxo species was proposed to be responsible for all subsequent chemistry. The extra electron needed for reductive cleavage of the peroxy bond is provided by ascorbate (or more precisely the semidehydroascorbate radical) *via* an outer sphere mechanism. Abstraction of an electron or hydrogen atom from the amine by the iron(IV)–oxo species would give a nitrogen based radical, which after rapid radical rearrangement would eventually result in cyclopropane ring cleavage and product formation.[129] This mechanism differs from the one proposed by Rocklin *et al.* Transient kinetic studies showed that ethylene was produced in a single turnover of the enzyme without ascorbate present. In this case, the substrate provides the electron for reductive O–O bond cleavage and reduction of the metal center comes at the end of the reaction cycle.[132] The two possible mechanisms are shown in Fig. 20.[132] In accord with the experimental data, a DFT study on ACCO concluded that the Fe(II)–acc–O_2 complex alone is not capable of generating any radical on the substrate and that a one-electron reduction of the metal complex is required. The computational results then, however, suggested that the actual reactive oxidizing species capable of generating the nitrogen-based substrate radical was an iron(II)–superoxo species and not the isoenergetic iron(III)–hydroperoxide species.[136]

Recently, the crystal structures of apo- and Fe(II)-complexed ACCO from *Petunia hybrida* were reported,[134] confirming the coordination of the iron(II) metal center by the 2-His-1-carboxylate facial triad with a monodentate aspartate residue. These structures provide a solid structural basis for future studies on this convoluted system.

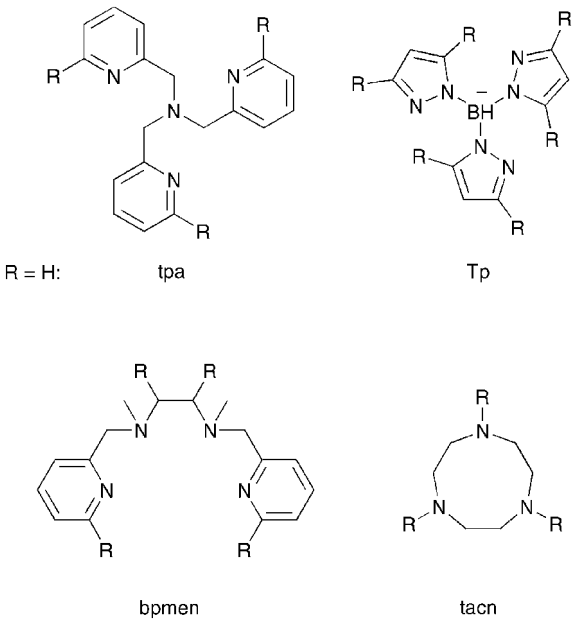

Fig. 21 Prominent polydentate all-*N* ligands that have been used in modeling studies of the enzymes with the 2-His-1-carboxylate facial triad. The R groups are drawn at positions, which are commonly modified.

4. Modeling studies

Many efforts by synthetic inorganic chemists have been devoted to biomimetic modeling studies of the enzymes of the 2-His-1-carboxylate facial triad family. Initial studies focused on the development of functional models of the different subfamilies and employed mostly polydentate all-*N* ligands. Impressive results have been obtained in the modeling of several of the different subfamilies (*vide infra*). The tris(2-pyridylmethyl)amine (tpa), hydridotris(pyrazol-1-yl)borato (Tp), *N*,*N*-bis(2-pyridylmethyl)-*N*,*N*′-dimethyl-1,2-ethylenediamine (bpmen) and 1,4,7-triazacyclononane (tacn) ligands and derivatives thereof have been used as the workhorses in many of these studies (Fig. 21).[7]

4.1 Structural models

Recently, attention has shifted to the design of structural models that more faithfully reproduce the coordination environment of the 2-His-1-carboxylate facial triad. Different approaches have been taken to mimic the facial coordination of two imidazole groups and a mono- or bidentate carboxylato group. Burzlaff and co-workers have studied the iron and zinc coordination chemistry of the bispyrazolylacetates,[137,138] which belong to the family of monoanionic *N*,*N*,*O*-heteroscorpionates.[139] The tripodal ligand framework of the bispyrazolylacetates predisposes the three donor groups to facially cap a metal center. The ligands are readily synthesized and the steric properties of the ligand can be varied by the introduction of pyrazole groups with different substitution patterns. Depending on the steric demand of the ligand and the nature of the iron precursor that is used different complexes have been obtained. The most common one is of the $[Fe^{II}L_2]$ type (Fig. 22A), but also a dimeric species with a bridging acetato group (B) and a mononuclear anionic ferric complex have been reported (C).[137,138] A ruthenium(II) complex of bis(3,5-dimethylpyrazol-1-yl)acetate with a bidentate α-keto acid benzoylformate has also been reported as a model for the α-ketoglutarate-dependent oxygenases.[140] Recent reports focused on the synthesis of chiral members and an enantiopure heteroscorpionate was reported.[141]

Que, Tolman and co-workers have communicated recently on a different synthetic strategy to obtain mononuclear iron(II) complexes with an *N*,*N*,*O*-donor set.[142] The use of a highly sterically hindered monodentate carboxylato ligand and a bulky diamine allowed the isolation of the mononuclear iron complex $[Fe^{II}Cl(BmaCO_2)(tBu_2Me_2eda)]$ (Fig. 23, left). The structure reveals a carboxylato ligand coordinated in a bidentate fashion, a coordination mode that is found in some of the enzymes with the 2-His-1-carboxylate structural motif. This bidentate binding mode of the carboxylate group is difficult to achieve with tripodal, tridentate chelates, such as the bis(pyrazolyl- or imidazolyl)acetates[137] or propionates[143] (*vide infra*). The chloride anion in $[Fe^{II}Cl(BmaCO_2)(tBu_2Me_2eda)]$ could be metathesized for other anions, which shows that despite all the steric bulk the iron center is still accessible and that functional modeling studies are feasible.

Recently, another mononuclear iron(II) complex $[Fe^{II}(\mathbf{L})Cl]$ has been reported with a bidentate carboxylate (Fig. 23, right).[144] The new polydentate ligand was built on the backbone of Kemp's acid and provides the iron with two pyridine *N* donors and one bidentate carboxylate. The iron complex

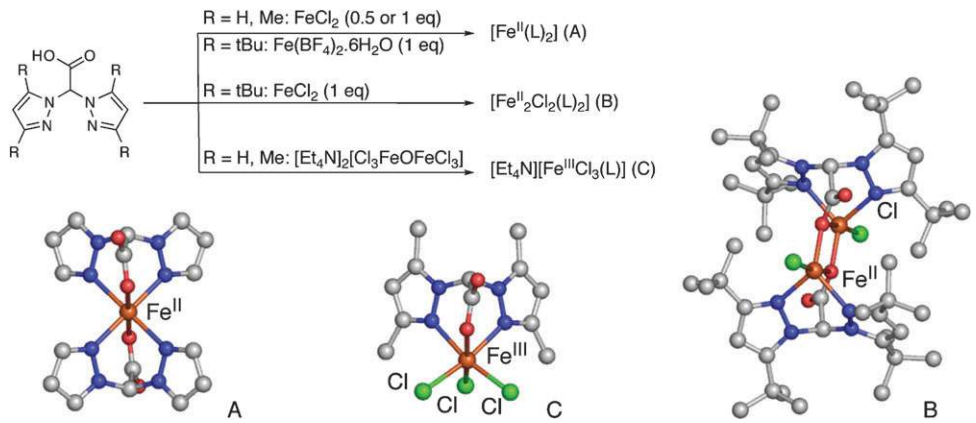

Fig. 22 Iron coordination chemistry of the substituted bispyrazolylacetato ligand family.

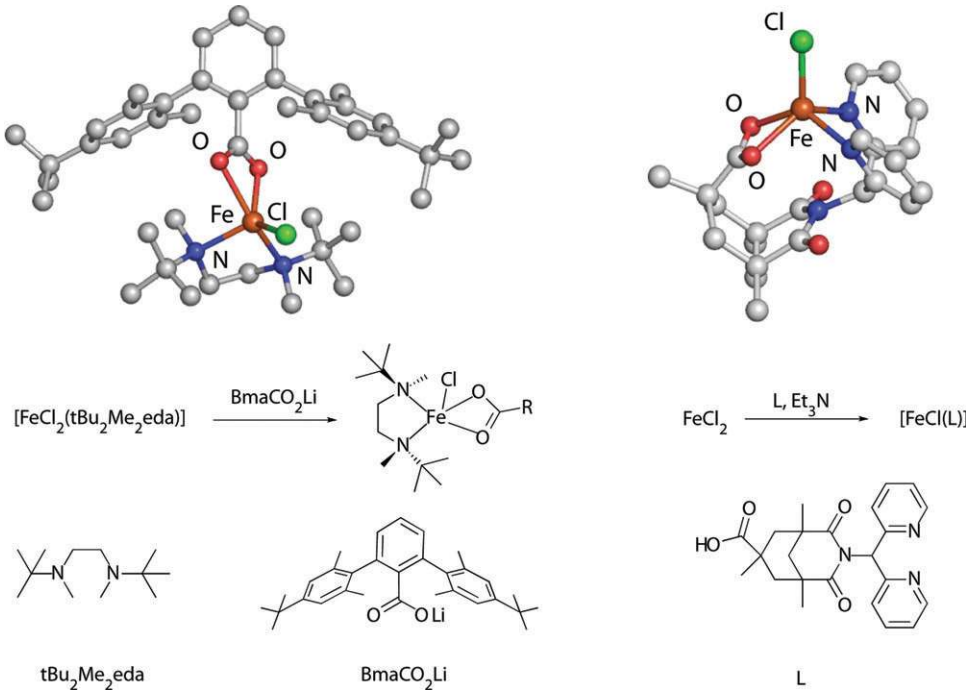

Fig. 23 Two mononuclear iron complexes with a bidentate coordination mode of the carboxylate moiety. Left: Assembly of a mononuclear iron complex from sterically hindered *N*- and *O*-ligands. Right: A structural and functional model of the Rieske dioxygenases with a new ligand based on the backbone of Kemp's acid.

thus approximates the 2-His-1-carboxylate environment encountered in, for instance, the Rieske dioxygenases. The model also displays *cis*-dihydroxylation activity with hydrogen peroxide (*vide infra*), albeit with less than one turnover.[144]

The nitrogen donor atoms in these structural models are distinctly different from those of the biological systems. The pyrazole rings of the bispyrazolylacetates, for instance, differ both in size, and in chemical and electronic properties from the histidyl imidazole-side chain found in the biological systems. To resemble also the electronic properties of the facial triad more closely a new tripodal ligand system was developed by the group of Klein Gebbink[143] and that of Burzlaff.[145] The family of substituted 3,3-bis(1-alkylimidazol-2-yl)propionates incorporates the biologically relevant 1-methylimidazole and carboxylato donor groups into a tripodal, monoanionic framework (Fig. 24). The facial capping potential of these ligands was initially illustrated by their copper,[143] rhenium, and manganese[145] complexes. Recently, the iron complexes $[Fe(MIm_2Pr)_2]$ with the parent ligand 3,3-bis(1-methylimidazol-2-yl)propionate (MIm_2Pr) and $[Fe(MIm_2PrPr)_2](X)_2$ (X = OTf, BPh_4) with its neutral propyl ester analogue propyl 3,3-bis(1-methylimidazol-2-yl)propionate (MIm_2PrPr) have also been reported.[146]

At the active site of the enzymes with the 2-His-1-carboxylate facial triad, the iron(II) center is facially capped by the three protein residues and the other three sites are either vacant or taken by solvent molecules. This situation is difficult to reproduce in a model system. Indeed, both with the bispyrazolylacetates[137] and 3,3-bis(1-alkylimidazol-2-yl)-propionates[146] often coordinatively saturated $[FeL_2]$ type complexes are obtained. Weckhuysen, Klein Gebbink and co-workers have reported a possible solution to this problem

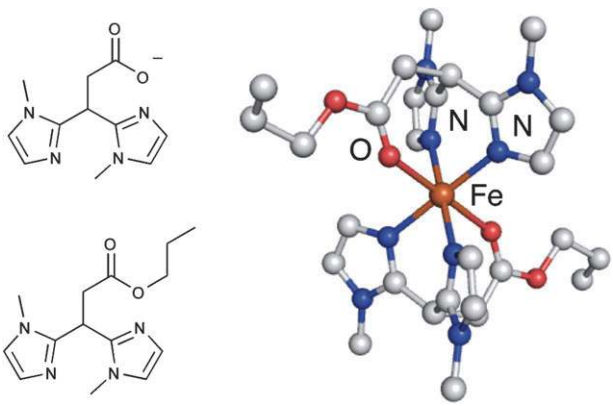

Fig. 24 The monoanionic, tripodal *N*,*N*,*O* binding ligand family of substituted 3,3-bis(1-methylimidazol-2-yl)propionates and an iron complex with the isopropyl ester analogue (anion omitted for clarity).

by immobilizing a 1 : 1 copper(II) complex with 3,3-bis-(1-methylimidazol-2-yl)propionate in a zeolite supercage. Spectroscopic studies revealed this species to be a five-coordinate metal complex facially capped by the tridentate *N*,*N*,*O*-ligand and coordinated by oxygen atoms from the zeolite Y lattice (Fig. 25).[147] The complex is catalytically active in the oxidation of benzyl alcohol. The mononuclearity of the complex, which is difficult to achieve in solution, was furthermore illustrated by the lack of activity in the oxidation of catechols, a reaction that typically requires two copper centers in close proximity. This strategy thus allowed the isolation of species in the zeolite superstructure that are not accessible in solution.

Klein Gebbink and co-workers also reported recently the first examples of homogeneous, mononuclear iron(II/III)

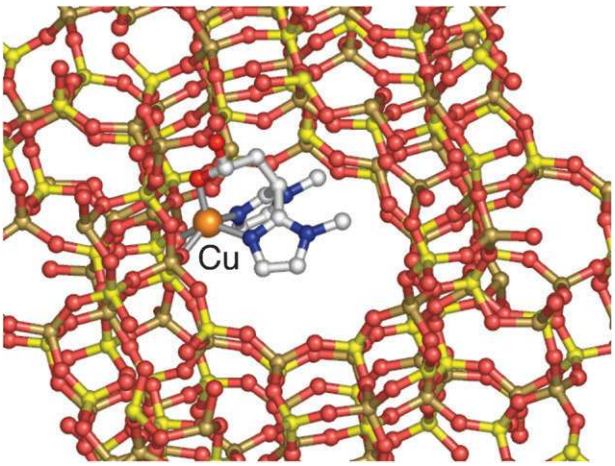

Fig. 25 Zeolite-immobilized copper(II) complex with the parent ligand 3,3-bis(1-methylimidazol-2-yl)propionate.

complexes of the substituted 3,3-bis(1-alkylimidazol-2-yl)-propionates.[148] Iron–catecholato complexes were reported as mimics of the enzyme–substrate complex of the extradiol cleaving dioxygenases (Fig. 26). The crystallographically characterized complex [Fe(EtiPrIm$_2$Pr)(tcc)(H$_2$O)] (tcc, tetrachlorocatechol) shows that the structural features of the facial triad are accurately captured by the ligand. Exposure of the complexes with 3,5-di-*tert*-butylcatechol as coligand to dioxygen resulted in (partial) extradiol type cleavage of the catechol. The complexes thus provide the first example of an accurate biomimetic model that incorporates both structural and functional properties.

4.2 Functional models

The efforts of synthetic chemists and their studies of the structure and reactivity of these functional models have provided much insight into the mechanistic details of the enzymes under scrutiny. Whereas most of the reports on iron complexes with a mixed donor set ligand have been limited to the structural aspects of the new complexes, functional models of all four major subfamilies of the facial triad have been developed as well, until recently mostly with all-*N* ligands.[79] In

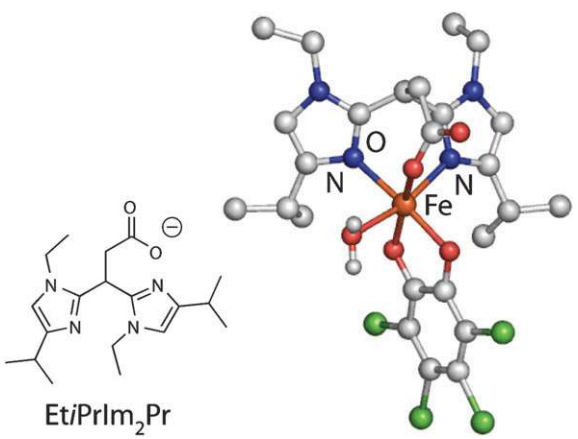

Fig. 26 A structural and functional model of the extradiol cleaving catechol dioxygenases of an *N*,*N*,*O*-tridentate monoanionic 3,3-bis-(1-alkylimidazol-2-yl)propionate ligand.

the following section we have mainly focused our discussion on those functional modeling studies specifically aimed at elucidating and modeling (specific steps) of the reactions of the enzymes under scrutiny. Indeed, in some cases the functional models do not turnover the enzyme's native substrate or they do not use dioxygen as the terminal oxidant, but the models nonetheless provide invaluable information about the mechanism of the enzyme and the intermediates involved. In this light, the large body of literature on bio-inspired oxidation catalysts[149] is beyond the scope of this section and will not be reviewed.

Several *ferrous α-keto acid complexes* have been reported with the tpa and Tp ligand systems as models of the enzyme-cofactor complex of the α-ketoglutarate-dependent oxygenases.[150–153] Crystal structural analyses have shown that the α-keto acids can coordinate to the metal center as a monodentate or bidentate ligand. Only the latter binding mode, however, gives rise to the typical chromophore that is also observed for the binary enzyme–cofactor complexes. These characteristic features in the visible were found to be sensitive to the nature of the α-keto acids, the supporting ligand and the coordination number of the iron center.

Most of these complexes show decarboxylation of the α-keto acid upon exposure to dioxygen, albeit with reaction rates differing largely.[151,153] The rate of oxygenation was found to be dependent on the coordination number of the complex, *i.e.* five-coordinate Tp (N_3) complexes reacted much faster than the six-coordinate tpa (N_4) complexes, illustrating the importance of a vacant site for dioxygen binding.[7,151] However, the sterically congested complex [Fe^{II}(bf)(Tp^{iPr,iBu})] (bf, benzoylformate) was found not to react, despite having a coordinatively unsaturated iron center.[152] Furthermore, the rate of oxidative decarboxylation was found to increase with more electron-withdrawing substituents on the α-keto acids. This supports the proposal of the involvement of an initial nucleophilic attack by an iron(III)–superoxo species on the α-keto acid co-substrate.[153]

In two cases the oxidative decarboxylation was also coupled to substrate oxidation. Valentine and co-workers showed that the complex [Fe(bf)(Tp^{Me_2})(MeCN)] could effect olefin epoxidation[151] and Que and co-workers reported the intramolecular aromatic hydroxylation of one of the phenyl substituents on Tp^{Ph_2} of [Fe(bf)(Tp^{Ph_2})(MeCN)] upon reaction with dioxygen (same reaction with other α-keto acids).[153] Isotope labeling studies using $^{18}O_2$ showed that one labeled oxygen atom was incorporated in the hydroxylated phenyl ring of the ligand and one in benzoic acid, thus mimicking the dioxygenase nature of the enzymes for the first time (Fig. 27A). The corresponding complexes bearing a carboxylate instead of an α-keto acid ligand also react with dioxygen to give the hydroxylated product, but this reaction proceeded two orders of magnitude slower, emphasizing the key role of the α-keto functionality in oxygen activation.[153]

The reported intramolecular arene hydroxylation is very similar to and in fact anticipated the observed enzyme self-inactivation by self-hydroxylation of an active site aromatic amino acid residue in the absence of substrate.[86]

In an attempt to mimic the chemistry of 4-hydrophenylpyruvate dioxygenase (*vide supra*), the iron coordination

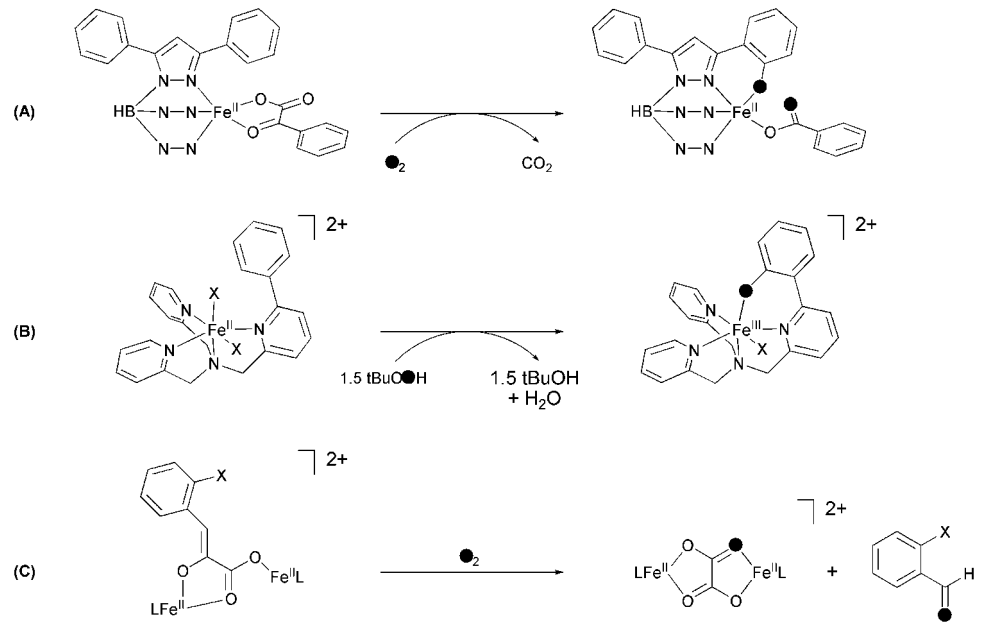

Fig. 27 Intramolecular arene hydroxylations that mimic the reactivities of the α-ketoglutarate (A) and pterin (B) dependent oxygenases. In one particular case, a different reactivity is observed when phenylpyruvate is used as the α-keto acid (C).

chemistry of the α-keto acid phenylpyruvate was studied and the dioxygen reactivity was found to be dependent on the supporting ligand.[154] With the tridentate Tp^{Ph_2} ligand the expected monoanionic, bidentate coordination mode of the α-keto acid and subsequent oxidative decarboxylation coupled with intramolecular hydroxylation were observed. In an interesting twist, however, an unexpected dinuclear iron complex with a tridentate dianionic bridging phenylpyruvate enolate was obtained with the tetradentate 6-Me_3-tpa ligand. Reaction with dioxygen now resulted in cleavage of the C2–C3 rather than the C1–C2 bond of the α-keto acid to give oxalate and benzaldehyde (Fig. 27C).[154] A subsequent detailed study of the structural characteristics and the reactivity of these and other iron complexes with phenylpyvurate has recently been reported.[155]

Similar *intramolecular arene hydroxylations* by mononuclear iron complexes have been observed as well.[7,156,157] A notable previous example, amongst others, is the reaction of *tert*-butylhydroperoxide with $[Fe(6\text{-Ph-tpa})(MeCN)_2]$ (6-Ph-tpa, phenyl appended tpa) (Fig. 27B).[156] The *ortho*-hydroxylated product is characterized by a phenolato-to-iron(III) LMCT band at 780 nm. The hydroxylation of the phenyl ring was proposed to proceed *via* electrophilic attack of the appended arene ring by a high valent iron(IV)–oxo species, similar to the proposed substrate oxidation step in the mechanism of the pterin-dependent monooxygenases. The (unobserved) high valent iron(IV)–oxo species would result from O–O bond homolysis of an observed Fe–OO^{t}Bu intermediate. Labeling experiments showed that the phenolate oxygen is derived from the terminal peroxide oxygen of ^{t}BuOOH *via* a species that can undergo partial oxygen exchange with water. This latter observation also points to the formation of an iron(IV)–oxo species as the reactive intermediate.[156] These biomimetic studies thus provided credence to the involvement of iron(IV)–oxo species in the oxidation reactions mediated by the pterin-dependent monooxygenase enzymes.

A recent example of an iron-promoted oxidation of a coordinated ligand is the regiospecific oxygen-atom insertion into iron(III) complexes of carboxylate-containing pentadentate ligand systems based on *N*-carboxymethyl-*N*′-R-*N*,*N*′-bis(2-pyridylmethyl)-1,2-ethanediamine (R = Me, Bn) (Fig. 28).[158] The reaction of these complexes with H_2O_2 or ^{t}BuOOH resulted in the incorporation of a single oxygen atom into the ligand producing a coordinated phenolato group (in case of the benzyl R-group) or an unprecedented coordinated N-oxide group (R = methyl). The reaction is evidenced by the evolution of dark blue color after addition of the oxidant in the case of the aromatic oxygenation, consistent with a phenolato-to-iron(III) LMCT band. Both products containing the two differently oxygenated ligands have been characterized crystallographically (Fig. 28). Based on some experimental observations and comparison with related systems, the authors suggest that the mechanism of oxygenation involves O–O bond heterolysis of an $[LFe^{III}OOR]^+$ species to give an $[LFe^{V}O]^{2+}$ species as the reactive intermediate.[158] Neither the $[LFe^{III}OOR]^+$ nor the $[LFe^{V}O]^{2+}$ intermediate has been, however, as of yet directly observed.

An oxoiron(V) intermediate has also been implicated in an *intermolecular aromatic hydroxylation* reaction. Perbenzoic acids were found to be converted to the corresponding salicylates when reacted with $[Fe(tpa)(CH_3CN)_2]^{2+}$.[159] Although an oxoiron(IV) species was detected spectroscopically, it was shown that this species could not be the actual oxidizing species, since a combination of independently prepared $[(tpa)Fe^{IV}{=}O]^{2+}$ did not result in any salicylate formation upon addition of benzoate. It was then proposed that the $[(tpa)Fe^{IV}{=}O]^{2+}$ is involved in the activation of a second perbenzoic acid in a subsequent step, thus forming an $[(tpa)Fe^{V}{=}O(benzoate)]^{3+}$ species which then hydroxylates the coordinated benzoate to salicylate.[159]

Similarly, the *ortho*-hydroxylation of benzoic acid to salicylic acid could also be achieved by the combination of

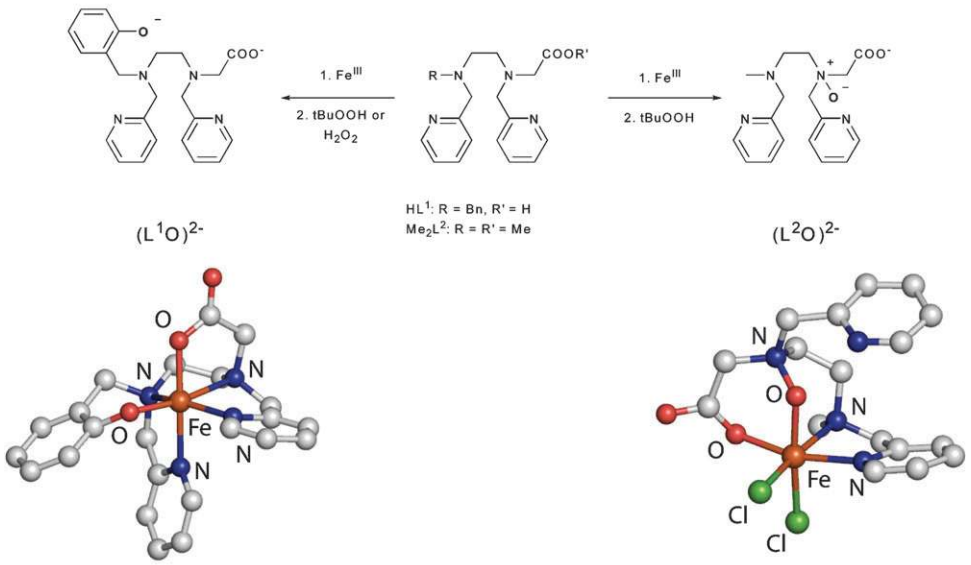

Fig. 28 Regiospecific ligand oxygenations in iron complexes of a carboxylate-containing ligand with H_2O_2 or ^{t}BuOOH.

mononuclear iron complex $[Fe^{II}(bpmen)(CH_3CN)_2]^{2+}$ and hydrogen peroxide.[160] In this case, a two-step reactivity was proposed as well. In the first step, the ferrous complex is oxidized by H_2O_2 to a ferric–hydroxide complex. The latter then reacts with a second equivalent of H_2O_2 to form an iron(III)–hydroperoxide. This intermediate could either directly hydroxylate the coordinated benzoate or undergo subsequent O–O bond cleavage to yield a high-valent iron–oxo species. Labeling studies were consistent with the hydroperoxide oxidant, but could not rule out a high-valent iron–oxo oxidant.[160]

Numerous modeling studies have been devoted to the *ring cleaving catechol dioxygenases*.[7,161] Intradiol type catechol cleavage is reported in by far the majority of cases, whereas examples of biomimetic systems capable of extradiol type catechol cleavage are actually quite limited.[7] The first functional models of the catechol dioxygenases were presented by Funabiki *et al.*, who reported oxidative catechol cleavage products with the combination of $FeCl_2$ or $FeCl_3$ and pyridine/bipyridine.[162] This reaction mixture resulted in significant amounts of both intradiol and extradiol type cleavage. In these and many of the later studies, 3,5-di-*tert*-butylcatechol was used as the substrate. The observed substituted 2-pyrones were recognized as the products of extradiol type cleavage and are believed to derive from decarbonylation of the extradiol-cleavage intermediate α-keto lactone.[162] In this pioneering study, the active species in this complicated mixture could, however, not be readily discerned and future studies, therefore, focused on the reactivity of isolated (mostly ferric) iron–catecholato complexes of the type [Fe(dtbc)(L)] (dtbc, 3,5-di-*tert*-butylcatecholato dianion). Most of these complexes are constructed with tetradentate ligands such as tpa, which results in coordinatively saturated iron–catecholato complexes. The complex $[Fe^{II}(6\text{-}Me_3\text{-}tpa)(dtbcH)]$ was the first reported mononuclear ferrous iron(II)–catecholato complex.[150] This complex accurately captured the monoanionic binding of the catechol, as observed only in the extradiol cleaving enzymes, but the lack of an available coordination site for O_2 rendered the complex susceptible for oxidation *via* an outer-sphere mechanism. Indeed, fast oxidation to the corresponding ferric complex $[Fe^{III}(6\text{-}Me_3\text{-}tpa)(dtbc)]$ and subsequent intradiol type cleavage was observed. The crystal structure of $[Fe^{II}(6\text{-}Me_2\text{-}bpmcn)(dtbcH)]$ also features a asymmetrically bound catecholato monoanion (Fig. 29A).[163]

It was recognized that the availability of a free coordination site was key to the observation of extradiol type cleavage and subsequent efforts focused on iron–catecholato complexes with tridentate ligands. Indeed, the highest selectivity for extradiol cleavage is generally obtained with tridentate, facially coordinating ligands such as tacn,[164,165] Me_3-tacn,[166] and Tp,[167] which illustrates not only the importance of such a vacant site at the metal center, but also the proper orientation of this vacant site with respect to the substrate. This coordination geometry is imposed by the ancillary ligand and is a key factor for determining the regioselectivity of the reaction. Indeed, iron–catecholato complexes with meridionally coordinating tridentate ligands such as terpyridine yielded no extradiol type products. In this case mainly the commonly observed autooxidation byproduct 3,5-di-*tert*-butylbenzoquinone and some intradiol type products were observed.[166] In contrast, $[Fe^{III}Cl(Me_3\text{-}tacn)(dtbc)]$ (Fig. 29C) with the facially coordinating tridentate Me_3-tacn ligand resulted in quantitative oxidation towards extradiol cleavage after abstraction of the chloride with a silver salt to generate an empty coordination site.[166] This observation furthermore illustrated that extradiol cleavage can be mediated by a ferric ion and does not necessarily require a ferrous metal center. The reactivity of these ferric complexes can be attributed to the partial iron(II)–semiquinone character of these complexes, which results from the low energy catecholato-to-iron charge transfer transitions characteristic for these type of complexes. However, Bugg and co-workers reported that the combination of $FeCl_2$/tacn was more selective towards extradiol cleavage than $FeCl_3$/tacn (7 : 1 and 2 : 1, respectively),[164] a finding consistent

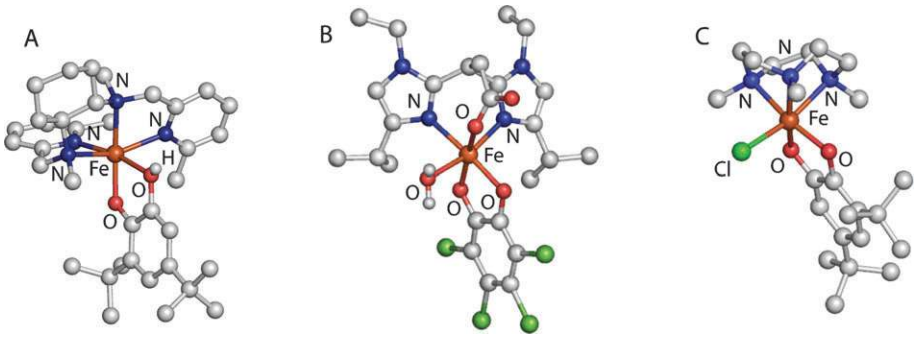

Fig. 29 Model complexes for the extradiol cleaving catechol dioxygenases. The ferrous structural model [Fe^{II}(6-Me_2-bpmcn)(dtbcH)] (A) excellently models the monoanionic, asymmetric binding of the catechol. The functional ferric models [Fe(EtiPrIm$_2$Pr)(tcc)(H_2O)] (B) and [Fe^{III}Cl(Me_3-tacn)(dtbc)] (C) are constructed with tridentate ligands. B accurately captures the facial triad and C exclusively affords extradiol type cleavage products.

with the presence of a ferrous ion at the enzyme active site. The use of catechol as the substrate in these experiments resulted in the first observation of the authentic extradiol ring fission product 2-hydroxymuconic aldehyde.[168] Replacement of one of the nitrogen donor atoms by oxygen, as in the enzyme active site, however, resulted in loss of activity.[164] An apparent exception to the observed requirement of a facially coordinating, tridentate ligand (or at least potentially tridentate after dissociation of one of the donor atoms in case of some tetradentate ligands) for extradiol type cleavage is the complex [Fe(LN_4H_2)(dtbc)] with the macrocyclic tetradentate ligand 2,11-diaza[3,3](2,6) pyridinophane (LN_4H_2), which gives a roughly equimolar mixture of intradiol and extradiol products after reaction with dioxygen.[169]

The first example of extradiol type cleavage with a complex built with a mixed donor set ligand similar to the 2-His-1-carboxylate facial triad was reported by Klein Gebbink and co-workers (Fig. 29B).[148] The ligands used in this study are the tridentate, tripodal, and monoanionic substituted 3,3-bis (1-alkylimidazol-2-yl)propionates, which provide the metal center with the biologically relevant imidazole and carboxylate groups. The iron complexes are coordinatively unsaturated in non-coordinating media and have a vacant coordination site accessible for Lewis bases, *e.g.* pyridine, or small molecules such as dioxygen. Ferrous complexes [Fe(L)(dtbcH)] with these ancillary *N*,*N*,*O*-ligands converted upon exposure to dioxygen to the corresponding ferric [Fe(L)(dtbc)] complexes within seconds, similarly to the few other characterized mononuclear iron(II)–catecholato complexes.[150,167] This was followed by a much slower second oxidation step that resulted in the oxidation of the catecholic substrate. The product distribution was found to be strongly solvent-dependent. In strongly coordinating solvents full conversion to the auto-oxidation quinone product was observed. In dichloromethane considerable amounts of oxidative cleavage products were observed. Although still about 45% of the catechol was converted into the quinone, extradiol and intradiol type cleavage products accounted for the remainder and were obtained in roughly equal amounts.[148] The few complexes reported thus far that are able to elicit extradiol cleavage also mediate concomitant intradiol cleavage, at least to some extent. The only synthetic complex that exclusively affords extradiol products is [Fe^{III}(Me_3-tacn)(dtbc)], but this system seems to be quite exceptional.[148,164] This suggests similar mechanisms for the two reactions and points at subtle influences on the ultimate product selectivity. Indeed, the mechanisms proposed for both types of enzymes converge on a common alkylperoxo intermediate,[7,28,29] which was recently directly detected in the extradiol cleaving enzyme homoprotocatechuate 2,3-dioxygenase (*vide supra*).[37] Both Bugg and co-workers[148,164] and Klein Gebbink and co-workers[144] noticed an increase in the yield of extradiol type product upon addition of a proton donor to the reaction mixture. This observation supports the hypothesis that the acid–base chemistry of a fully conserved second sphere protonated histidine residue in the extradiol cleaving enzymes is key to the fate of the alkylperoxo intermediate and subsequently the regiospecificity of the cleavage.[36,38,40]

The functional models described above in most cases display stoichiometric, so-called 'single turnover' reactivities. Functional modeling studies on the Rieske dioxygenases, however, have actually resulted in the discovery of a family of *catalysts capable of cis-dihydroxylation*.[170] Ferrous complexes of the ligands tpa and bpmen provided the first example of *cis*-dihydroxylation catalyzed by a non-biological iron complex,[171] a reaction that usually requires reagents such as OsO_4. All complexes in this family are six-coordinate with a tripodal (tpa) or linear (bpmen) tetradentate N_4 ligand. The remaining (*cis*-positioned) coordination sites are occupied by labile ligands such as acetonitrile. The electronic and steric properties of the ligand environment could be altered by attaching alkyl substituents to the pyridine rings of the ligands, which modulated the spin state of the complexes. Even enantioselective *cis*-dihydroxylation with an ee up to 82% has been reported using a chiral analogue of bpmen.[172] The complexes use hydrogen peroxide as oxidant and catalyze the oxidation of a range of olefins with high efficiency. At the same time, these complexes catalyze olefin epoxidation and the actually observed epoxide to *cis*-diol ratios differ widely amongst the reported examples.[170] These two reactions are closely related and the availability of two *cis*-positioned vacant sites was proposed as a necessary requirement for both types of reactivities.[63] The product ratio was found to be dependent on the adopted ligand topology and the spin state of the metal

center.[63,173] These factors influence the fate of an implicated Fe^{III}–OOH intermediate such that low spin intermediates generally yield more epoxide and high-spin intermediates more *cis*-diol. This iron(III)–hydroperoxide is formed by an initial one-electron oxidation of the ferrous complex to an Fe^{III}–OH species. The latter species then reacts with more H_2O_2 to generate the olefin oxidation catalyst.[63] Depending on the spin-state of this intermediate, two pathways have been proposed, *i.e.* a water-assisted (wa) pathway for the epoxide selective catalysts and a non-water-assisted (nwa) pathway for the diol selective catalysts (Fig. 30).[63,170]

Isotopic labeling studies using either $H_2{}^{18}O$ or $H_2{}^{18}O_2$ have proven particularly insightful and the mechanistic considerations rely heavily on the results obtained from these experiments. Labeling experiments suggest that in the wa-pathway O–O cleavage must occur prior to substrate oxidation and hence a HO–Fe^{V}=O oxidant is proposed. This high-valent oxoiron(V) species is derived from the experimentally observed Fe^{III}–OOH intermediate. The low-spin iron center of this species weakens and activates the O–O bond.[170] Pre-equilibrium water binding to the adjacent vacant site further activates the hydroperoxide and promotes O–O bond heterolysis by the formation of a hydrogen-bonded five-membered ring species.[63] The thus generated HO–Fe^{V}=O oxidant would allow for incorporation of oxygen atoms from both the oxidant and water in both the epoxide and *cis*-dihydroxylation products, consistent with the isotopic labeling studies. DFT computational studies are consistent with the proposed wa pathway and furthermore suggest that epoxidation or *cis*-dihydroxylation results from initial attack of the olefin by the oxide or hydroxide of the common HO–Fe^{V}=O oxidant, respectively.[174]

The mechanism of the nwa-pathway is less clear and direct attack of the olefin by the Fe^{III}–OOH intermediate has been suggested.[175] Labeling experiments show that both oxygen atoms in the *cis*-diol product derive from one single molecule of H_2O_2. The nature of the oxidants in the two different pathways thus differs significantly. Competition experiments have furthermore shown that the oxidant in the wa-pathway has an electrophilic character (preferentially oxidizing the more electron-rich olefins), whereas in the nwa-pathway a nucleophilic oxidant (oxidizing the more electron-deficient olefins) is generated.[176] The observed electrophilic character in the wa-pathway is consistent with the proposed HO–Fe^{V}=O oxidant.

In addition to the tpa and bpmen complexes and derivatives thereof, other complexes capable of *cis*-dihydroxylation have also been reported (Fig. 31).[146,177–179] The iron complex derived from N3py-R reported by Feringa and co-workers shows comparable reactivity to the original tpa and bmpen systems.[177] Interestingly, the stereoselectivity of the reaction was solvent-dependent in this particular case, *i.e. cis*- or *trans*-diol was obtained from acetonitrile or acetone solutions, respectively. ^{18}O Labeling studies in acetonitrile are in agreement with the mechanistic scheme detailed above. In acetone, however, labeling studies suggested that the solvent is the likely source of one of the oxygens in the *trans*-diol product and thus is actively involved in a competing mechanistic pathway.[177] A mixture of *cis*- and *trans*-diol products was also observed, in addition to epoxide formation, in the anaerobic oxidation of cyclooctene with a bispidine-iron(II)/H_2O_2 system in acetonitrile.[180] In contrast to the previous systems, the ancillary ligand is a pentadentate N_5 ligand. In this case, the diol formation was proposed to arise from yet another pathway not previously observed in non-heme iron-based oxidation catalysis. A low-spin iron(III)–hydroperoxide intermediate is believed to undergo homolysis of the O–O bond, yielding an oxoferryl species and a hydroxide radical. Attack of the substrate by [Fe^{IV}=O] yields a radical species which can recombine with the hydroxide radicals to give a mixture of *cis*- and *trans*-diols.[180]

Recently, examples have been reported that use tridentate ligands with an *N*,*N*,*O*-donor set to more closely mimic the site of the mononuclear iron center in the Rieske dioxygenases (Fig. 31). Oldenburg *et al.* use the ligand Ph-dpah, which

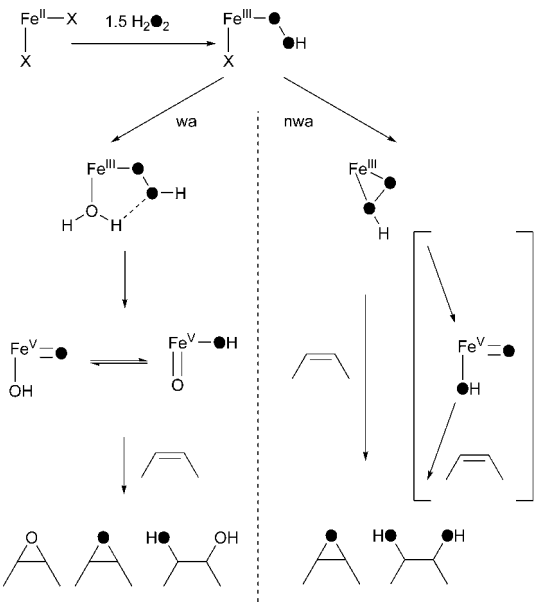

Fig. 30 Proposed pathways for the oxidation of olefins by non-heme iron catalysts.

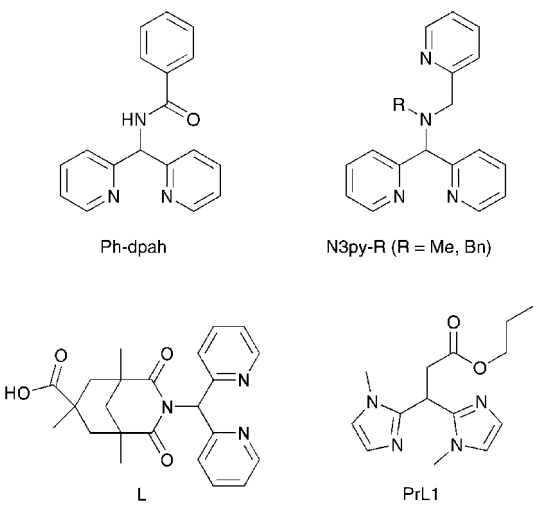

Fig. 31 Ligands featured in iron olefin epoxidation and *cis*-dihydroxylation catalysts.

features an amide carbonyl atom as the oxygen donor atom, to obtain the most selective *cis*-dihydroxylation catalyst reported to date.[178] The ferrous complex $[Fe^{II}(Ph\text{-}dpah)_2](OTf)_2$ is centrosymmetric with two facially coordinated ligands resulting in a six-coordinate iron center. Although coordinatively saturated, the complex is an excellent olefin *cis*-dihydroxylation catalyst, oxidizing a range of olefins. To account for the observed reactivity, complete dissociation of one ligand to give three sites available for exogenous ligand binding was proposed.[178] The observation of both doubly (64%) and singly (33%) labeled *cis*-diols lead to the proposal of an $Fe^{V}(O)(OH)(OH_2)$ intermediate as the oxidizing species.[178]

In a related contribution, Klein Gebbink and co-workers showed that iron complexes of the neutral propyl ester analogue of 3,3-bis(1-methylimidazol-2-yl)propionate (MIm_2PrPr) also show good epoxidation and *cis*-dihydroxylation activity.[146] Two different coordination modes of the ligand were observed. In $[Fe(MIm_2PrPr)_2](OTf)_2$ the ligands are facially coordinated with an *N*,*N*,*O*-donor set similar to the complex $[Fe^{II}(Ph\text{-}dpah)_2](OTf)_2$, whereas in $[Fe(MIm_2PrPr)_2(MeOH)_2](OTf)_2$ a bidentate *N*,*N*-binding of the ligands results in a complex more similar to the tpa derived iron complexes. Despite the overall structural resemblance between $[Fe(MIm_2PrPr)_2](OTf)_2$ and $[Fe^{II}(Ph\text{-}dpah)_2](OTf)_2$, there is a remarkable difference in product selectivity in olefin oxidation as $[Fe(MIm_2PrPr)_2](OTf)_2$ seems to slightly favor epoxidation.[146] As in the Rieske dioxygenases, the polydentate ligand L (3-(dipyridin-2-yl-methyl)-1,5,7-trimethyl-2,4-dioxo-3-aza-bicyclo[3.3.1]nonane-7-carboxylate) in the mononuclear iron(II) complex $[Fe^{II}(L)Cl]$ provides the metal with a bidentate carboxylate rather than carbonyl oxygen donor atoms as in the previous two mimics.[144] Less than one turnover of product was obtained in the $[Fe^{II}(L)Cl]$ mediated oxidation of olefins and mainly epoxidation was observed with traces of *cis*-diol formation. The small yields of diol were attributed to partial loss of the chloride during the reaction to generate the required *cis*-positioned labile sites. Indeed, removal of the chloride ligand with silver triflate resulted in a dramatic change from 50 : 1 (Cl) in favor of epoxide to 1 : 6 (OTf) in favor of the diol in the oxidation of 1-octene with H_2O_2, although again with less than one turnover of product. Labeling studies showed that the oxygen atoms of the diol product were derived from one molecule of H_2O_2, demonstrating that the system serves as an exemplary dioxygenase model.[144]

The insights obtained from enzymology and functional models have played an important role in the design of bio-inspired oxidation catalysts. The family of *cis*-dihydroxylation/epoxidation catalysts mentioned before is just one example of many biomimetic, non-heme iron oxidation catalysts that use hydrogen peroxide as the oxidant. The recent report of Chen and White on the selective C–H oxidation of a broad range of substrates, which even include complex natural products, by a small molecule non-heme iron oxidation catalyst illustrates the tremendous potential of such systems as a synthetic method in organic chemistry.[181] This topic is, however, beyond the scope of this review and has furthermore been reviewed very recently and will therefore not be discussed here.[149]

5. Reaction intermediates

In many of the studies of both the enzymes and the model systems discussed above iron–(hydro)peroxide and/or high-valent iron(IV)–oxo or iron(V)–oxo intermediates are invoked. Several efforts have been specifically devoted to the study, isolation and characterization of these species to get more insight into the spectroscopic and chemical properties of these intermediates. These studies are discussed below.

5.1 Iron(III)–hydroperoxide and –peroxide species

Iron(III)–hydroperoxide ($Fe^{III}OOH$) and iron(III)–peroxide ($Fe^{III}O_2$) species are often suggested as intermediates between the initial binding of dioxygen to iron and the formation of the actual, active oxidant in many different heme and non-heme iron biomolecules.[7] Examples for the latter category include, for instance, the crystallographically observed side-on bound peroxide adduct of naphthalene dioxygenase.[52] In the Rieske dioxygenases, the group of enzymes to which naphthalene dioxygenase belongs, this intermediate has been proposed by some authors to be the actual oxidant rather than a precursor to a high valent iron–oxo oxidant (*vide supra*).[15,61] The crystal structure of an end-on bound iron(III)–(hydro)peroxide intermediate has also been recently reported for the first time.[182] Three different peroxide species were actually observed in three of the four subunits of the crystallographic homotetramer. All of these were bound in an end-on fashion and were studied further by '*in crystallo*' Raman spectroscopy affording valuable structural and geometric parameters. The intermediates were trapped in the crystal of superoxide reductase, a non-heme iron enzyme in which the metal center is coordinated by four histidines and a cysteinate ligand. Superoxide reductase converts the toxic superoxide radical anion into hydrogen peroxide.

Since the first report of the generation of an $Fe^{III}OOH$ intermediate with a model compound by Mascharak and co-workers,[183] a number of mononuclear, non-heme iron(III)–(hydro)peroxide complexes have been constructed with different, mostly neutral, polydentate ligands such as N4py,[184] tpa,[185] H_2bbpa,[186] Rtpen,[187] and bispidine-derived[188] ligands (Fig. 32).[7,189] These species are usually generated by the reaction of an iron(II) precursor with H_2O_2 at low temperatures. They have been characterized by a variety of spectroscopic techniques including resonance Raman, UV-Vis, EPR, Mössbauer and XAS spectroscopy and by mass spectrometric methods.[184,187,189–191]

A crystallographically characterized example of a biomimetic mononuclear non-heme iron(III)–(hydro)peroxide is, however, still lacking. The only example of an iron(III) complex with a coordinated peroxide group is the peroxocarbonate complex $[Ph_4P][Fe^{III}(\kappa_2\text{-}CO_4)(quin)_2]$ that results from the reaction of an iron–hydroperoxide precursor with carbon dioxide (Fig. 33, top).[192] The iron–hydroperoxide intermediate was obtained from the reaction of the diferric complex $[Fe_2(quin)_2(OH)_2]$ with hydrogen peroxide in the presence of base. The study of the peroxocarbonate complex also provided the first example of reversible O–O bond cleavage and formation of a peroxide group involving an iron(III) complex, which is proposed to proceed through an high-valent iron–oxo species.[193]

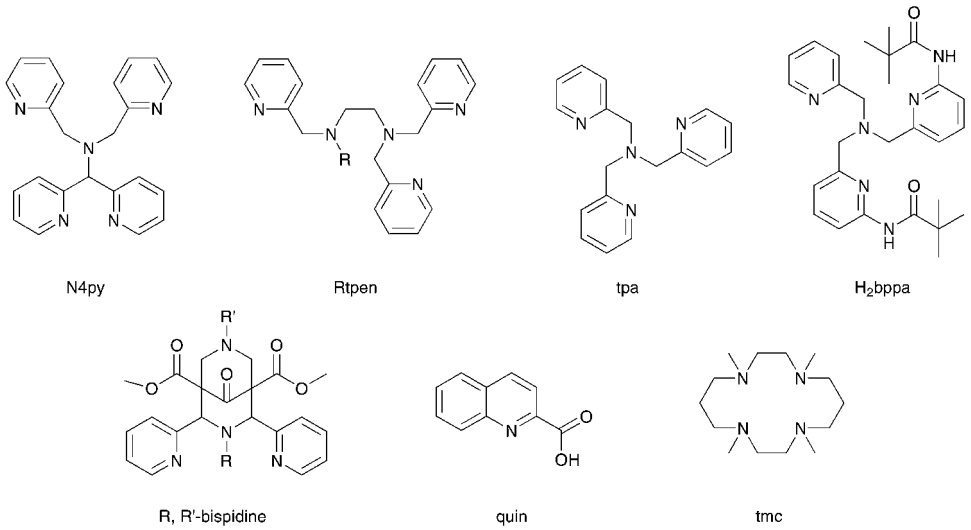

Fig. 32 Some selected ligand systems that have been used to generate iron(III)–(hydro)peroxide complexes.

The initially formed $[Fe^{III}(\eta^1\text{-OOH})(L)]^{n+}$ complexes are generally low-spin ($S = 1/2$), purple-blue species with one LMCT absorption in the visible region at about 550–600 nm. High spin $[Fe^{III}(\eta^1\text{-OOH})(L)]^{n+}$ complexes have also been obtained with the sterically hindered H_2bppa ligand and the anionic quin ligand (Fig. 32).[186,192] Isotope-sensitive Raman vibrations around $\sim$600 and $\sim$800 cm^{-1} are characteristic for these iron–hydroperoxide species, with the low-spin complex generally displaying higher ν_{Fe-O} and lower ν_{O-O} frequencies than their high-spin counterparts.[7,185,186] These observations suggest that coordination to a low spin ferric center weakens the peroxide bond and strengthens the Fe–O bond.[186]

Some complexes, such as for example $[Fe^{III}(\eta^1\text{-OOH})(N4py)]^{2+}$,[184,194] but not all,[188] show reversible acid–base chemistry (Fig. 33, bottom). The addition of base, such as NH_3 (aq), results in the formation of the conjugate base of the complex. A side-on bound η^2-peroxide structure is proposed for the conjugate base, based on resonance Raman, Mössbauer, and DFT studies (Fig. 33, bottom).[184,188] The $[Fe^{III}(\eta^2\text{-}O_2)(L)]^{(n-1)+}$ complexes are high-spin ($S = 5/2$) ferric complexes and display a red-shifted electronic transition compared to their protonated counterparts. The Raman spectra show a shift of $\sim$20 cm^{-1} of the ν_{O-O} vibration to higher frequency and the $\nu_{(Fe-O_2)}$ vibration is found just below 500 cm^{-1}. Addition of perchloric acid reverses the reaction and restores the hydroperoxide species.[195] For side-on bound peroxide complexes with the pentadentate N_5 ligands, either a seven-coordinate structure or a six-coordinate complex formed by the dissociation of one of the nitrogen donors could be envisaged to accommodate the η^2-O_2 moiety. The significantly different properties of side-on peroxo complexes with differently substituted bispidine ligands point to the formation of seven-coordinate iron–peroxo complexes,[188] as was suggested before.[184,194]

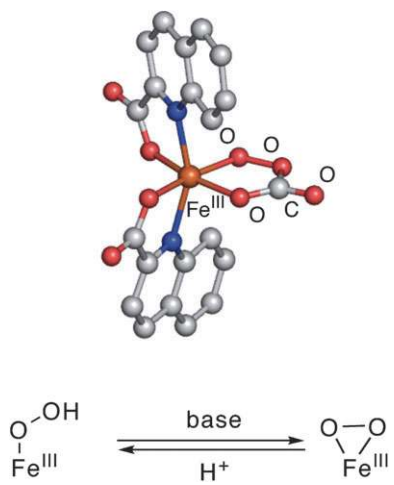

Fig. 33 Top: Only available molecular structure of a mononuclear iron complex with a peroxide group $[Ph_4P][Fe^{III}(quin)_2(\kappa_2\text{-}CO_4)]$. Bottom: Edge-on $[Fe^{III}(\eta^1\text{-OOH})]^{n+}$ to side-on $[Fe^{III}(\eta^2\text{-}O_2)]^{(n-1)+}$ conversion.

In addition to the study of the structural characteristics of these ferric (hydro)peroxides, establishing the reactivity of these intermediates itself is essential as well, since in some cases these species have been suggested to be the actual oxidant rather than a precursor to an oxidizing species resulting from subsequent O–O bond cleavage.[196] Initial reactivity studies already showed that the side-on $[Fe^{III}(\eta^2\text{-}O_2)(N4py)]^{+}$ complex was relatively unreactive compared to its edge-on $[Fe^{III}(\eta^1\text{-OOH})(N4py)]^{2+}$ counterpart towards alkane substrates.[195] This difference was attributed to the former species being incapable of activating the O–O bond. The low reactivity is consistent with the electronic description of a side-on bound peroxide to a ferric metal center, which indicates no activation or weakening of the O–O bond.[2]

The reactivities of both the edge-on hydroperoxide and side-on peroxide complexes *themselves* were studied by the reaction between previously well-characterized, *in situ* generated complexes and stoichiometric amounts of various substrates at temperatures at which the (hydro)peroxide intermediates are stable.[196] $[Fe^{III}(\eta^2\text{-}O_2)]^{(n-1)+}$ complexes were found to be active in a typical nucleophilic oxidation reaction as the complex $[Fe^{III}(\eta^2\text{-}O_2)(tmc)]^{+}$ was found to be active in the deformylation of aldehydes.[196,197] No reactivity

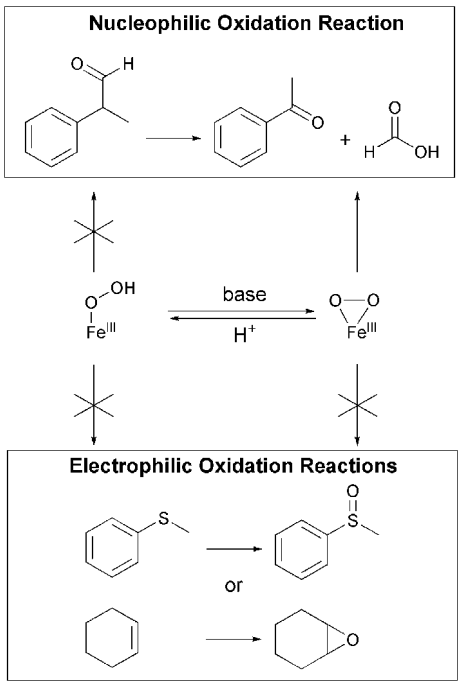

Fig. 34 Reactivity of mononuclear non-heme hydroperoxo– and peroxo–iron intermediates in typical nucleophilic and electrophilic oxidation reactions.

was, however, observed in typical electrophilic oxidation reactions, such as the oxidation of sulfide or olefin (Fig. 34).

The same study showed that several different $[Fe^{III}(\eta^1\text{-OOH})]^{n+}$ complexes were not capable of deformylating aldehydes at low temperatures nor were they active in electrophilic reactions such as sulfide and olefin oxidation (Fig. 34).[196] Substrate conversion was only observed upon warming of the reaction mixtures. These results indicate that an $[Fe^{III}(\eta^1\text{-OOH})]^{n+}$ complex seems a sluggish oxidant as well and, therefore, can not be the active species in sulfoxidation, epoxidation or alkane hydroxylation reactions.[196]

5.2 High-valent non-heme iron–oxo species

In many of the above reactions catalyzed by enzymes with the 2-His-1-carboxylate facial triad and in model systems, a high-valent iron(IV)–oxo intermediate has been implicated as the reactive oxidizing species. Such species have been characterized previously in several heme-containing iron enzymes and more recently it has been detected directly in the α-ketoglutarate-dependent mononuclear non-heme iron enzymes as well. A high-valent iron(IV)–oxo species was first observed in the mononuclear non-heme iron enzyme TauD.[17] A combination of stopped-flow absorption and freeze-quench Mössbauer spectroscopies together with resonance Raman and X-ray absorption experiments allowed the assignment of the detected intermediate as an iron(IV)–oxo with a high-spin $S = 2$ configuration. Such an intermediate has been subsequently detected in prolyl-4-hydroxylase[21] and in the related α-keto acid dependent halogenase CytC3, in which the asp/glu ligand of the triad is absent to create a site for halide coordination.[22] In a recent contribution, spectroscopic evidence for a high-spin Fe(IV) species has also been reported for a different subfamily of the 2-His-1-carboxylate facial triad, as the hydroxylating intermediate in the pterin-dependent enzyme tyrosine hydroxylase was trapped and characterized with stopped-flow absorption and freeze-quench Mössbauer spectroscopies.[110] These important findings show that this species is also viable in an enzyme with a non-heme iron active site.

At the same time, synthetic efforts were aimed at the development of model systems with an Fe(IV)=O group with the aim of setting chemical precedents for the biochemical transformations.[25] A chronological perspective that led to the isolation and characterization of the first such species has been recently given by Que.[198] In 2000, the first evidence for such a species in a mononuclear non-heme iron environment was presented, albeit in low yield.[199] Subsequently, in a landmark paper in 2003 Que and co-workers presented the high-yield synthesis and spectroscopic properties of the non-heme iron complex $[Fe^{IV}(O)(tmc)(MeCN)](OTf)_2$ with a terminal iron-(IV)–oxo species.[24] The remarkable stability of this species even allowed crystallization and subsequent determination of a high-resolution crystal structure of the complex (Fig. 35). After this initial report, several more examples have appeared of iron(IV)–oxo complexes. The crystal structure of one of these, $[Fe^{IV}(O)(N4py)](ClO_4)_2$ has also been determined.[23]

These results incited many experimental and theoretical studies[25,200] into the spectroscopic properties,[201–203] coordination chemistry[204,205] and reactivity[193,206–208] of these high-valent iron complexes. Several routes have been developed to obtain the desired high-valent complexes. These generally involve the reaction of an iron(II) precursor with oxidants like peracids,[209] iodosylbenzene,[24] peroxides,[210] and even an example has been reported that uses dioxygen[211] as the oxidant. In other cases, the species is obtained by decomposition of an alkyl- or hydroperoxo species by O–O bond homolysis.[210,212] A recent survey of results that implicate or establish the involvement of oxoiron(IV) species in biomimetic oxidations is available.[25]

The pale-green species are generally characterized by an electronic absorption with low-intensity in the near-IR region. This spectroscopic signature has been proven to be very convenient for the detection of such species and was found to be quite sensitive to alterations in the ligand environment of the mononuclear iron center. An MCD analysis of $[Fe^{IV}(O)(tmc)(MeCN)](OTf)_2$ showed that these bands were

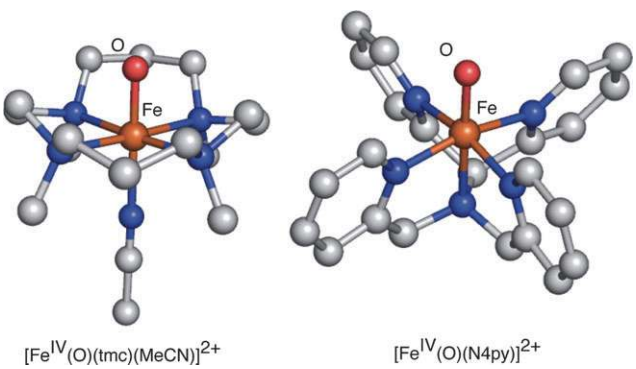

Fig. 35 Molecular structures of the cations of the two crystallographically characterized Fe(IV)=O complexes.

associated with ligand field transitions expected of a low-spin iron(IV) center with C_{4v} symmetry.[201] Further characteristics are a short Fe–O bond of 1.646 and 1.636 Å for $[Fe^{IV}(O)(tmc)(MeCN)](OTf)_2$ and $[Fe^{IV}(O)(N4py)](ClO_4)_2$, respectively, and Mössbauer parameters characteristic of an $S = 1$ ground state.[25] The latter feature contrasts with the high-spin $S = 2$ detected in the enzymes and can be attributed to the stronger ligand field that is brought about by the all-*N* ligands in the model complexes compared to the weaker ligand field exerted by the 2-His-1-carboxylate ligand combination. A noticeable exception is the (only) $S = 2$ Fe(IV)=O complex generated the reaction of $[Fe(H_2O)_6]^{2+}$ with ozone in acidic aqueous media (*vide infra*).[213] DFT calculations correlate well with the experimental description of these species and show that the electronic structure of the iron–oxo unit is dominated by very strong and highly covalent interactions.[200] The thermal stabilities of these complexes differ widely, ranging from seconds to days at room temperature.[198] The complexes with nonplanar tetradentate ligands tpa and bpmcn, for instance, are much less stable than the complexes with the macrocyclic, planar tmc ligand or the pentadentate N4py ligand. Another interesting and somewhat counterintuitive observation[198] is the decrease in thermal stability that is observed when *cis*-monoanionic ligands are introduced in oxoiron(IV) complexes of tpa.[204]

Recently, the formation of iron(IV)–oxo complexes in aqueous solution under various conditions has been reported.[202,213,214] The generation of such a species and the study of its reactivity provided critical insight into the nature of the oxidant in the classical Fenton reaction, *i.e.* the reaction between Fe^{II} and H_2O_2 in water. An Fe(IV)=O species has sometimes been invoked as an alternative to the hydroxyl radical as the reactive oxidant, but studies on the reactivity of iron(IV)–oxo complexes under Fenton conditions unambiguously ruled out the involvement of this species as the actual oxidant.[213]

With the structure of the non-heme iron(IV)–oxo species firmly established by the crystallographic results described above, the reactivity of these complexes was subsequently tested in various reactions. The reactivity of mononuclear non-heme iron–oxo complexes in oxygenation reactions is discussed in a recent account.[215] The first evidence for oxygen atom transfer by a non-heme iron(IV)–oxo species was provided by the quantitative oxidation of triphenylphosphine to triphenylphosphine oxide by $[Fe(O)(tmc)]^{2+}$.[24] The complexes were also found to be active in, for instance, alkane hydroxylation,[206,216] olefin epoxidation,[206,209] alcohol oxidation,[217] sulfide oxidation[211,218] and oxidative N-dealkylations[219] (Fig. 36). The latter reactivity, for instance, mimics the reactivity of the *Escherischia coli* AlkB protein, an α-ketoglutarate-dependent non-heme iron enzyme that plays an important role in alkylated DNA damage repair and for which a high-valent iron–oxo species has been proposed as the oxidizing species.[73]

The complex $[Fe^{IV}(O)(N4py)](ClO_4)_2$ was even found to be capable of oxidizing the unactivated C–H bonds of cyclohexane at room temperature.[216] This result shows that the Fe(IV)=O unit has sufficient oxidizing power to cleave aliphatic C–H bonds[216] and it has been calculated to be even more

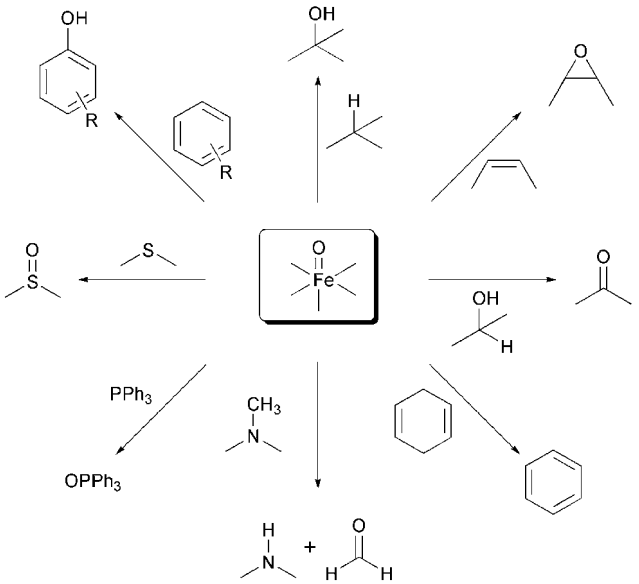

Fig. 36 Diversity in oxidation reactions mediated by non-heme Fe(IV) complexes (adapted from Nam[215]).

reactive than the corresponding iron(IV)–oxo porphyrin cation radical of P450 (Compound I).[220] Furthermore, a large KIE of >30 was observed in the hydroxylation of ethylbenzenes, which implies that the C–H bond activation by these iron(IV)–oxo species occurs *via* a hydrogen atom abstraction mechanism. Similarly large KIEs were observed in H-abstraction reactions catalyzed by TauD.[88]

Whereas in all reported systems artificial oxidants such as peracids, iodosylarenes and hydroperoxides were used in the oxidation reactions, in one case catalytic oxidation of several organic substrates was brought about by using dioxygen as the primary oxidant. The reaction of $[Fe^{II}(tmc)(OTf)_2]$ with dioxygen in a solvent mixture of acetonitrile and butyl ether resulted in the formation of an oxoiron(IV) intermediate capable of oxidizing PPh_3, thioanisole and benzyl alcohol without the need to add an external reductant.[211]

In many studies, the incorporation of labeled oxygen (^{18}O) from isotopically labeled water ($H_2{}^{18}O$) into oxidation products has been considered as evidence for the involvement of high-valent Fe(IV)=O intermediates in oxygen-atom transfer reactions. Nam and co-workers provided direct evidence for the oxygen-atom exchange between non-heme oxoiron(IV) complexes and isotopically labeled water and reported the direct measurement of the rates and activation parameters of this important oxygen exchange reaction.[208] In addition, Nam and co-workers reported the intermetal transfer of oxygen between non-heme iron complexes. The transfer of oxygen from an iron(IV)–oxo to an iron(II) complex was found to be dependent on the oxidizing power of the iron(IV)–oxo complex.[207]

The development, characterization, and reactivity studies on biomimetic iron(IV)–oxo complexes has provided strong credence to the mechanisms proposed for the non-heme iron enzymes.

A high valent Fe(V)=O oxidant has been proposed by some authors for the oxygen activation mechanism of the Rieske dioxygenases only (*vide supra*).[7] In contrast to the structurally

characterized Fe(IV)=O species, no direct evidence has been reported yet for the proposed HO–Fe(V)=O oxidant. Mechanistic studies, in particular isotopic labeling experiments, on bio-inspired *cis*-dihydroxylation[170] and alkane hydroxylation catalysts,[177,221] however, strongly implicate the involvement of such an oxidant in these systems. The involvement of an iron(V)–oxo has also been suggested in the self-hydroxylation of different perbenzoic acids by a non-heme iron complex[159] and in a regioselective ligand oxidation.[158]

Experimentally observed low-molecular weight iron(V) models are, however, exceedingly rare. Wieghardt and co-workers reported a mononuclear non-heme iron(V)–nitrido complex, which was generated by the photolysis of an azidoiron(III) precursor.[222,223] In an exciting recent development, the first chemical and spectroscopic evidence for an Fe^{V}–oxo complex was reported.[26] The reaction of the $[PPh_4][Fe^{III}(taml)(H_2O)]$ with the oxygen donor *m*-chloroperbenzoic acid resulted in the nearly quantitative synthesis of a green species, which was identified as $[Fe(taml)(O)]^{-}$. Mass spectrometry, Mössbauer, EPR and X-ray absorption (Fe K-edge and EXAFS) spectroscopies all pointed to the formulation of $[Fe(taml)(O)]^{-}$ as a genuine iron(V)–oxo species. The deprotonated tetraamido macrocyclic ligand (taml) offers four exceptionally strong amido-N σ-donors to the iron, which allows for the stabilization of the high-valent Fe^{V}–oxo complex.[26] The long-lived species is stable over a month at 77 K. The iron(V)–oxo was found to exhibit a low spin ($S = 1/2$) d^3 configuration. Its chemical reactivity furthermore characterized it as a strongly oxidizing iron–oxo complex capable of oxo-transfer, including oxygen atom insertion reaction into C–H bonds, and electron-transfer reactions. These results show that such high-valent iron–oxo species can be obtained in a non-heme iron environment and as such provide credence to the mechanism involving iron(V)–oxo intermediates proposed for the Rieske dioxygenases.[7] Furthermore, the iron–taml systems are efficient green oxidation catalysts, capable of decomposing of numerous pollutants.[224,225] The characterized $Fe^{V}(O)$ species is the likely reactive intermediate in these reactions.[26]

6. Concluding remarks

The recent explosion in crystallographically characterized non-heme iron enzymes has firmly established the 2-His-1-carboxylate facial triad as a common platform for dioxygen activation in Nature. The breadth of oxidative transformations is stunning and many reactions do not have a precedent in synthetic organic chemistry. New members of the family are reported at a remarkable pace, which illustrates both the ubiquity and the versatility of the triad. This holds great promise for the future and without doubt new systems that mediate exciting new chemistry will be discovered. In terms of mechanistic understanding of these reactivities, great strides have been made by complementary, parallel studies of enzymes and their biomimetic model complexes, with notable achievements such as the detection and crystallization of iron(IV)–oxo species. Many questions still remain, however, that concern the steps that follow initial dioxygen binding and lead to product formation. The elaborate studies of synthetic functional analogues have contributed greatly to our understanding of these enzymes. The recent developments towards the synthesis of even more precise high-fidelity structural and functional models promise further progress in this field and may ultimately lead to the development of synthetically useful catalysts.

Acknowledgements

The authors gratefully thank the National Research School Combination Catalysis (NRSC-C) for financial support.

References

1 M. M. Abu-Omar, A. Loaiza and N. Hontzeas, *Chem. Rev.*, 2005, **105**, 2227.
2 E. I. Solomon, T. C. Brunold, M. I. Davis, J. N. Kernsley, S.-K. Lee, N. Lehnert, F. Neese, A. J. Skulan, Y.-S. Yang and J. Zhou, *Chem. Rev.*, 2000, **100**, 235.
3 M. L. Neidig and E. I. Solomon, *Chem. Commun.*, 2005, 5843.
4 E. I. Solomon, P. Chen, M. Metz, S.-K. Lee and A. E. Palmer, *Angew. Chem., Int. Ed.*, 2001, **40**, 4570.
5 R. H. Holm, P. Kennepohl and E. I. Solomon, *Chem. Rev.*, 1996, **96**, 2239.
6 I. G. Denisov, T. M. Makris, S. G. Sligar and I. Schlichting, *Chem. Rev.*, 2005, **105**, 2253.
7 M. Costas, M. P. Mehn, M. P. Jensen and L. Que, Jr, *Chem. Rev.*, 2004, **104**, 939.
8 E. Y. Tshuva and S. J. Lippard, *Chem. Rev.*, 2004, **104**, 987.
9 K. D. Koehntop, J. P. Emerson and L. Que, Jr, *J. Biol. Inorg. Chem.*, 2005, **10**, 87.
10 E. L. Hegg and L. Que, Jr, *Eur. J. Biochem.*, 1997, **250**, 625.
11 L. Que, Jr, *Nat. Struct. Biol.*, 2000, **7**, 182.
12 S. V. Kryatov, E. V. Rybak-Akimova and S. Schindler, *Chem. Rev.*, 2005, **105**, 2175.
13 E. G. Kovaleva and J. D. Lipscomb, *Nat. Chem. Biol.*, 2008, **4**, 186.
14 K. Valegard, A. C. Terwisscha van Scheltinga, M. D. Lloyd, T. Hara, S. Ramaswamy, A. Perrakis, A. Thompson, H.-J. Lee, J. E. Baldwin, C. J. Schofield, J. Hajdu and I. Andersson, *Nature*, 1998, **394**, 805.
15 D. J. Ferraro, L. Gakhar and S. Ramaswamy, *Biochem. Biophys. Res. Commun.*, 2005, **338**, 175.
16 W. L. Delano, in *The Pymol Molecular Graphics System*, San Carlos, CA, 2002.
17 J. M. Bollinger, Jr, J. C. Price, L. M. Hoffart, E. W. Barr and C. Krebs, *Eur. J. Inorg. Chem.*, 2005, 4245.
18 J. C. Price, E. W. Barr, B. Tirupati, J. M. Bollinger, Jr and C. Krebs, *Biochemistry*, 2003, **42**, 7497.
19 D. A. Proshlyakov, T. F. Henshaw, G. R. Monterosso, M. J. Ryle and R. P. Hausinger, *J. Am. Chem. Soc.*, 2004, **126**, 1022.
20 P. J. Riggs-Gelasco, J. C. Price, R. B. Guyer, J. H. Brehm, E. W. Barr, J. M. Bollinger, Jr and C. Krebs, *J. Am. Chem. Soc.*, 2004, **126**, 8108.
21 L. M. Hoffart, E. W. Barr, R. B. Guyer, J. M. Bollinger, Jr and C. Krebs, *Proc. Natl. Acad. Sci. U. S. A.*, 2006, **103**, 14738.
22 D. P. Galonic, E. W. Barr, C. T. Walsh, J. M. Bollinger, Jr and C. Krebs, *Nat. Chem. Biol.*, 2007, **3**, 113.
23 E. J. Klinker, J. Kaizer, W. W. Brennessel, N. L. Woodrum, C. J. Cramer and L. Que, Jr, *Angew. Chem., Int. Ed.*, 2005, **44**, 3690.
24 J.-U. Rohde, J.-H. In, M. H. Lim, W. W. Brennessel, M. R. Bukowski, A. Stubna, E. Munck, W. Nam and L. Que, Jr, *Science*, 2003, **299**, 1037.
25 X. P. Shan and L. Que, *J. Inorg. Biochem.*, 2006, **100**, 421.
26 F. Tiago de Oliveira, A. Chanda, D. Banerjee, X. Shan, S. Mondal, L. Que, Jr, E. L. Bominaar, E. Munck and T. J. Collins, *Science*, 2007, **315**, 835.
27 C. D. Brown, M. L. Neidig, M. B. Neibergall, J. D. Lipscomb and E. I. Solomon, *J. Am. Chem. Soc.*, 2007, **129**, 7427.

28 F. H. Vaillancourt, J. T. Bolin and L. D. Eltis, *Crit. Rev. Biochem. Mol. Biol.*, 2006, **41**, 241.
29 T. D. H. Bugg and G. Lin, *Chem. Commun.*, 2001, 941.
30 L. Que, Jr and M. F. Reynolds, *Met. Ions Biol. Syst.*, 2000, **37**, 505.
31 F. H. Vaillancourt, C. J. Barbosa, T. G. Spiro, J. T. Bolin, M. W. Blades, R. F. B. Turner and L. D. Eltis, *J. Am. Chem. Soc.*, 2002, **124**, 2485.
32 M. I. Davis, E. C. Wasinger, A. Decker, M. Y. M. Pau, F. H. Vaillancourt, J. T. Bolin, L. D. Eltis, B. Hedman, K. O. Hodgson and E. I. Solomon, *J. Am. Chem. Soc.*, 2003, **125**, 11214.
33 E. L. Spence, G. J. Langley and T. D. H. Bugg, *J. Am. Chem. Soc.*, 1996, **118**, 8336.
34 S. L. Groce, M. A. Miller-Rodeberg and J. D. Lipscomb, *Biochemistry*, 2004, **43**, 15141.
35 S. L. Groce and J. D. Lipscomb, *Biochemistry*, 2005, **44**, 7175.
36 P. E. M. Siegbahn and F. Haeffner, *J. Am. Chem. Soc.*, 2004, **126**, 8919.
37 E. G. Kovaleva and J. D. Lipscomb, *Science*, 2007, **316**, 453.
38 S. Mendel, A. Arndt and T. D. H. Bugg, *Biochemistry*, 2004, **43**, 13390.
39 A. Viggiani, L. Siani, E. Notomista, L. Birolo, P. Pucci and A. Di Donato, *J. Biol. Chem.*, 2004, **279**, 48630.
40 S. L. Groce and J. D. Lipscomb, *J. Am. Chem. Soc.*, 2003, **125**, 11780.
41 D. T. Gibson and R. E. Parales, *Curr. Opin. Biotechnol.*, 2000, **11**, 236.
42 K. Furukawa, H. Suenaga and M. Goto, *J. Bacteriol.*, 2004, **186**, 5189.
43 Y. Jouanneau, C. Meyer, J. Jakoncic, V. Stojanoff and J. Gaillard, *Biochemistry*, 2006, **45**, 12380.
44 D. J. Ferraro, E. N. Brown, C. L. Yu, R. E. Parales, D. T. Gibson and S. Ramaswamy, *BMC: Struct. Biol.*, 2007, **7**, 10.
45 D. R. Boyd and T. D. H. Bugg, *Org. Biomol. Chem.*, 2006, **4**, 181.
46 D. T. Gibson, S. M. Resnick, K. Lee, J. M. Brand, D. S. Torok, L. P. Wackett, M. J. Schocken and B. E. Haigler, *J. Bacteriol.*, 1995, **177**, 2615.
47 P. L. Herman, M. Behrens, S. Chakraborty, B. M. Chrastil, J. Barycki and D. P. Weeks, *J. Biol. Chem.*, 2005, **280**, 24759.
48 J. Lee and H. Zhao, *Angew. Chem., Int. Ed.*, 2006, **45**, 622.
49 B. M. Martins, T. Svetlitchnaia and H. Dobbek, *Structure*, 2005, **13**, 817.
50 A. Pinto, M. Tarasev and D. P. Ballou, *Biochemistry*, 2006, **45**, 9032.
51 M. Tarasev, A. Pinto, D. Kim, S. J. Elliot and D. P. Ballou, *Biochemistry*, 2006, **45**, 10208.
52 A. Karlsson, J. V. Parales, R. E. Parales, D. T. Gibson, H. Eklund and S. Ramaswamy, *Science*, 2003, **299**, 1039.
53 B. Kauppi, K. Lee, E. Carredano, R. E. Parales, D. T. Gibson, H. Eklund and S. Ramaswamy, *Structure*, 1998, **6**, 571.
54 A. Karlsson, J. V. Parales, R. E. Parales, D. T. Gibson, H. Eklund and S. Ramaswamy, *J. Biol. Inorg. Chem.*, 2005, **10**, 483.
55 Y. Furusawa, V. Nagarajan, M. Tanokura, E. Masai, M. Fukuda and T. Senda, *J. Mol. Biol.*, 2004, **342**, 1041.
56 R. Friemann, M. M. Ivkovic-Jensen, D. J. Lessner, C. L. Yu, D. T. Gibson, R. E. Parales, H. Eklund and S. Ramaswamy, *J. Mol. Biol.*, 2005, **348**, 1139.
57 X. Dong, S. Fushinobu, E. Fukuda, T. Terada, S. Nakamura, K. Shimizu, H. Nojiri, T. Omori, H. Shoun and T. Wakagi, *J. Bacteriol.*, 2005, **187**, 2483.
58 H. Nojiri, Y. Ashikawa, H. Noguchi, J. W. Nam, M. Urata, Z. Fujimoto, H. Uchimura, T. Terada, S. Nakamura, K. Shimizu, T. Yoshida, H. Habe and T. Omori, *J. Mol. Biol.*, 2005, **351**, 355.
59 J. Jakoncic, Y. Jouanneau, C. Meyer and V. Stojanoff, *FEBS J.*, 2007, **274**, 2470.
60 Y. Ashikawa, Z. Fujimoto, H. Noguchi, H. Habe, T. Omori, H. Yamane and H. Nojiri, *Structure*, 2006, **14**, 1779.
61 A. Bassan, M. R. A. Blomberg and P. E. M. Siegbahn, *J. Biol. Inorg. Chem.*, 2004, **9**, 439.
62 A. Bassan, T. Borowski and P. E. M. Siegbahn, *Dalton Trans.*, 2004, 3153.
63 K. Chen, M. Costas, J. Kim, A. K. Tipton and L. Que, Jr, *J. Am. Chem. Soc.*, 2002, **124**, 3026.
64 S. Chakrabarty, R. N. Austin, D. Deng, J. T. Groves and J. D. Lipscomb, *J. Am. Chem. Soc.*, 2007, **129**, 3514.
65 M. D. Wolfe, J. V. Parales, D. T. Gibson and J. D. Lipscomb, *J. Biol. Chem.*, 2001, **276**, 1945.
66 M. Tarasev and D. P. Ballou, *Biochemistry*, 2005, **44**, 6197.
67 D. J. Ferraro, A. L. Okerlund, J. C. Mowers and S. Ramaswamy, *J. Bacteriol.*, 2006, **188**, 6986.
68 I. J. Clifton, M. A. McDonough, D. Ehrismann, N. J. Kershaw, N. Granatino and C. J. Schofield, *J. Inorg. Biochem.*, 2006, **100**, 644.
69 R. P. Hausinger, *Crit. Rev. Biochem. Mol. Biol.*, 2004, **39**, 21.
70 K. S. Hewitson, N. Granatino, R. W. D. Welford, M. A. McDonough and C. J. Schofield, *Philos. Trans. R. Soc. London, Ser. A*, 2005, **363**, 807.
71 V. Purpero and G. R. Moran, *J. Biol. Inorg. Chem.*, 2007, **12**, 587.
72 C. Krebs, D. Galonic Fujimori, C. T. Walsh and J. M. Bollinger, Jr, *Acc. Chem. Res.*, 2007, **40**, 484.
73 B. Yu, W. C. Edstrom, J. Benach, Y. Hamuro, P. C. Weber, B. R. Gibney and J. F. Hunt, *Nature*, 2006, **439**, 879.
74 Y. Mishina and C. He, *J. Inorg. Biochem.*, 2006, **100**, 670.
75 O. Sundheim, C. B. Vagbo, M. Bjoras, M. M. L. Sousa, V. Talstad, P. A. Aas, F. Drablos, H. E. Krokan, J. A. Tainer and G. Slupphaug, *EMBO J.*, 2006, **25**, 3389.
76 P. A. C. Cloos, J. Christensen, K. Agger, A. Maiolica, J. Rappsilber, T. Antal, K. H. Hansen and K. Helin, *Nature*, 2006, **442**, 307.
77 Y.-I. Tsukada, J. Fang, H. Erdjument-Bromage, M. E. Warren, C. H. Borchers, P. Tempst and Y. Zhang, *Nature*, 2006, **439**, 811.
78 C. J. Schofield and P. J. Ratcliffe, *Nat. Rev. Mol. Cell Biol.*, 2004, **5**, 343.
79 M. A. McDonough, V. Li, E. Flashman, R. Chowdhury, C. Mohr, B. M. R. Lienard, J. Zondlo, N. J. Oldham, I. J. Clifton, J. Lewis, L. A. McNeill, R. J. M. Kurzeja, K. S. Hewitson, E. Yang, S. Jordan, R. S. Syed and C. J. Schofield, *Proc. Natl. Acad. Sci. U. S. A.*, 2006, **103**, 9814.
80 E. G. Pavel, J. Zhou, R. W. Busby, M. Gunsior, C. A. Townsend and E. I. Solomon, *J. Am. Chem. Soc.*, 1998, **120**, 743.
81 J. R. O'Brien, D. J. Schuller, V. S. Yang, B. D. Dillard and W. N. Lanzilotta, *Biochemistry*, 2003, **42**, 5547.
82 E. G. Pavel, J. Zhou, R. W. Busby, M. Gunsior, C. A. Townsend and E. I. Solomon, *J. Am. Chem. Soc.*, 1998, **120**, 743.
83 J. M. Elkins, M. J. Ryle, I. J. Clifton, J. C. Dunning Hotopp, J. S. Lloyd, N. I. Burzlaff, J. E. Baldwin, R. P. Hausinger and P. L. Roach, *Biochemistry*, 2002, **41**, 5185.
84 K. Valegard, A. C. Terwisscha van Scheltinga, A. Dubus, G. Ranghino, L. M. Oster, J. Hajdu and I. Andersson, *Nat. Struct. Mol. Biol.*, 2004, **11**, 95.
85 I. Muller, A. Kahnert, T. Pape, G. M. Sheldrick, W. Meyer-Klaucke, T. Dierks, M. Kertesz and I. Uson, *Biochemistry*, 2004, **43**, 3075.
86 E. R. Farquhar, K. D. Koehntop, J. P. Emerson and L. Que, Jr, *Biochem. Biophys. Res. Commun.*, 2005, **338**, 230.
87 G. Schenk, M. Y. M. Pau and E. I. Solomon, *J. Am. Chem. Soc.*, 2004, **126**, 505.
88 J. C. Price, E. W. Barr, T. E. Glass, C. Krebs and J. M. Bollinger, Jr, *J. Am. Chem. Soc.*, 2003, **125**, 13008.
89 G. R. Moran, *Arch. Biochem. Biophys.*, 2005, **433**, 117.
90 O. W. Choroba, D. H. Wiliams and J. B. Spencer, *J. Am. Chem. Soc.*, 2000, **122**, 5389.
91 M. L. Neidig, A. Decker, O. W. Choroba, F. Huang, M. Kavana, G. R. Moran, J. B. Spencer and E. I. Solomon, *Proc. Natl. Acad. Sci. U. S. A.*, 2006, **103**, 12966.
92 F. H. Vaillancourt, E. Yeh, D. A. Vosburg, S. Garneau-Tsodikova and C. T. Walsh, *Chem. Rev.*, 2006, **106**, 3364.
93 F. H. Vaillancourt, J. Yin and C. T. Walsh, *Proc. Natl. Acad. Sci. U. S. A.*, 2005, **102**, 10111.
94 F. H. Vaillancourt, E. Yeh, D. A. Vosburg, S. E. O'Connor and C. T. Walsh, *Nature*, 2005, **436**, 1191.
95 M. Ueki, D. P. Galonic, F. H. Vaillancourt, S. Garneau-Tsodikova, E. Yeh, D. A. Vosburg, F. C. Schroeder, H. Osada and C. T. Walsh, *Chem. Biol.*, 2006, **13**, 1183.

96 D. P. Galonic, F. H. Vaillancourt and C. T. Walsh, *J. Am. Chem. Soc.*, 2006, **128**, 3900.
97 L. C. Blasiak, F. H. Vaillancourt, C. T. Walsh and C. L. Drennan, *Nature*, 2006, **440**, 368.
98 D. Galonic Fujimori, E. W. Barr, M. L. Matthews, G. M. Koch, J. R. Yonce, C. T. Walsh, J. M. Bollinger, C. Krebs and P. J. Riggs-Gelasco, *J. Am. Chem. Soc.*, 2007, **129**, 13408.
99 P. F. Fitzpatrick, *Annu. Rev. Biochem.*, 1999, **68**, 355.
100 T. Flatmark and R. C. Stevens, *Chem. Rev.*, 1999, **99**, 2137.
101 K. E. Goodwill, C. Sabatier, C. Marks, R. Raag, P. F. Fitzpatrick and R. C. Stevens, *Nat. Struct. Biol.*, 1997, **4**, 578.
102 B. Kobe, I. G. Jennings, C. M. House, B. J. Michell, K. E. Goodwill, B. D. Santarsiero, R. C. Stevens, R. G. H. Cotton and B. E. Kemp, *Nat. Struct. Biol.*, 1999, **6**, 442.
103 L. Wang, H. Erlandsen, J. Haavik, P. M. Knappskog and R. C. Stevens, *Biochemistry*, 2002, **41**, 12569.
104 O. A. Andersen, T. Flatmark and E. Hough, *J. Mol. Biol.*, 2001, **314**, 279.
105 H. Erlandsen, J. Y. Kim, M. G. Patch, A. Han, A. Volner, M. M. Abu-Omar and R. C. Stevens, *J. Mol. Biol.*, 2002, **320**, 645.
106 O. A. Andersson, T. Flatmark and E. Hough, *J. Mol. Biol.*, 2002, **320**, 1095.
107 A. Y. Han, A. Q. Lee and M. M. Abu-Omar, *Inorg. Chem.*, 2006, **45**, 4277.
108 J. P. Klinman, *J. Biol. Inorg. Chem.*, 2001, **6**, 1.
109 J. A. Pavon and P. F. Fitzpatrick, *Biochemistry*, 2006, **45**, 11030.
110 B. E. Eser, E. W. Barr, P. A. Frantom, L. Saleh, J. M. Bollinger, C. Krebs and P. F. Fitzpatrick, *J. Am. Chem. Soc.*, 2007, **129**, 11334.
111 J. A. Pavon and P. F. Fitzpatrick, *J. Am. Chem. Soc.*, 2005, **127**, 16414.
112 G. R. Moran, A. Derecskei-Kovacs, P. J. Hillas and P. F. Fitzpatrick, *J. Am. Chem. Soc.*, 2000, **122**, 4535.
113 P. A. Frantom and P. F. Fitzpatrick, *J. Am. Chem. Soc.*, 2003, **125**, 16190.
114 T. Urich, C. M. Gomes, A. Kletzin and C. Frazao, *Science*, 2006, **311**, 996.
115 Z.-W. Chen, C.-Y. Jiang, Q. She, S.-J. Liu and P.-J. Zhou, *Appl. Environ. Microbiol.*, 2005, **71**, 621.
116 T. Urich, A. Kroke, C. Bauer, K. Seyfarth, M. Reuff and A. Kletzin, *FEMS Microbiol. Lett.*, 2005, **248**, 171.
117 L. J. Higgins, F. Yan, P. Liu, H.-W. Liu and C. L. Drennan, *Nature*, 2005, **437**, 838.
118 Z. Zhao, P. Liu, M. Kazuo, T. Kuzuyama, H. Seto and H.-W. Liu, *Angew. Chem., Int. Ed.*, 2002, **41**, 4529.
119 P. Liu, A. Liu, F. Yan, M. D. Wolfe, J. D. Lipscomb and H.-W. Liu, *Biochemistry*, 2003, **42**, 11577.
120 F. Yan, J. W. Munos, P. Liu and H.-W. Liu, *Biochemistry*, 2006, **45**, 11473.
121 K. McLuskey, S. Cameron, F. Hammerschmidt and W. N. Hunter, *Proc. Natl. Acad. Sci. U. S. A.*, 2005, **102**, 14221.
122 P. Liu, M. P. Mehn, F. Yan, Z. Zhao, L. Que, Jr and H.-W. Liu, *J. Am. Chem. Soc.*, 2004, **126**, 10306.
123 N. J. Kershaw, M. E. C. Caines, M. C. Sleeman and C. J. Schofield, *Chem. Commun.*, 2006, 4251.
124 N. I. Burzlaff, P. J. Rutledge, I. J. Clifton, C. M. H. Hensgens, M. Pickford, R. M. Adlington, P. L. Roach and J. E. Baldwin, *Nature*, 1999, **401**, 721.
125 P. L. Roach, I. J. Clifton, C. M. H. Hensgens, N. Shibata, A. J. Long, R. W. Strange, S. S. Hasnain, C. J. Schofield, J. E. Baldwin and J. Hajdu, *Eur. J. Biochem.*, 1996, **242**, 736.
126 P. L. Roach, I. J. Clifton, C. M. H. Hensgens, N. Shibata, C. J. Schofield, J. Hajdu and J. E. Baldwin, *Nature*, 1997, **387**, 827.
127 A. Daruzzaman, I. J. Clifton, R. M. Adlington, J. E. Baldwin and P. J. Rutledge, *ChemBioChem*, 2006, **7**, 351.
128 A. J. Long, I. J. Clifton, P. L. Roach, J. E. Baldwin, P. J. Rutledge and C. J. Schofield, *Biochemistry*, 2005, **44**, 6619.
129 J. Thrower, L. M. Mirica, K. P. McCusker and J. P. Klinman, *Biochemistry*, 2006, **45**, 13108.
130 N. M. W. Brunhuber, J. L. Mort, R. E. Christoffersen and N. O. Reich, *Biochemistry*, 2000, **39**, 10730.
131 J. S. Thrower, R. Blalock, III and J. P. Klinman, *Biochemistry*, 2001, **40**, 9717.
132 A. M. Rocklin, K. Kato, H.-W. Liu, L. Que, Jr and J. D. Lipscomb, *J. Biol. Inorg. Chem.*, 2004, **9**, 171.
133 J. Zhou, A. M. Rocklin, J. D. Lipscomb, L. Que, Jr and E. I. Solomon, *J. Am. Chem. Soc.*, 2002, **124**, 4602.
134 Z. Zhang, J.-S. Ren, I. J. Clifton and C. J. Schofield, *Chem. Biol.*, 2004, **11**, 1383.
135 D. L. Tierney, A. M. Rocklin, J. D. Lipscomb, L. Que, Jr and B. M. Hoffman, *J. Am. Chem. Soc.*, 2005, **127**, 7005.
136 A. Bassan, T. Borowski, C. J. Schofield and P. E. M. Siegbahn, *Chem.–Eur. J.*, 2006, **12**, 8835.
137 A. Beck, A. Barth, E. Hubner and N. Burzlaff, *Inorg. Chem.*, 2003, **42**, 7182.
138 A. Beck, B. Weibert and N. Burzlaff, *Eur. J. Inorg. Chem.*, 2001, 521.
139 A. Otero, J. Fernandez-Baeza, A. Antinolo, J. Tejeda and A. Lara-Sanchez, *Dalton Trans.*, 2004, 1499.
140 R. Muller, E. Hubner and N. Burzlaff, *Eur. J. Inorg. Chem.*, 2004, 2151.
141 L. Peters and N. Burzlaff, *Polyhedron*, 2004, **23**, 245.
142 S. J. Friese, B. E. Kucera, L. Que, Jr and W. B. Tolman, *Inorg. Chem.*, 2006, **45**, 8003.
143 P. C. A. Bruijnincx, M. Lutz, A. L. Spek, E. E. van Faassen, B. M. Weckhuysen, G. van Koten and R. J. M. Klein Gebbink, *Eur. J. Inorg. Chem.*, 2005, 779.
144 P. D. Oldenburg, C.-Y. Ke, A. A. Tipton, A. A. Shteinman and L. Que, Jr, *Angew. Chem., Int. Ed.*, 2006, **45**, 7975.
145 L. Peters, E. Hubner and N. Burzlaff, *J. Organomet. Chem.*, 2005, **690**, 2009.
146 P. C. A. Bruijnincx, I. L. C. Buurmans, S. Gosiewska, M. Moelands, M. Lutz, A. L. Spek, G. van Koten and R. J. M. Klein Gebbink, *Chem.–Eur. J.*, 2008, **14**, 1228.
147 K. Kervinen, P. C. A. Bruijnincx, A. M. Beale, J. G. Mesu, G. van Koten, R. J. M. Klein Gebbink and B. M. Weckhuysen, *J. Am. Chem. Soc.*, 2006, **128**, 3208.
148 P. C. A. Bruijnincx, M. Lutz, A. L. Spek, W. R. Hagen, B. M. Weckhuysen, G. van Koten and R. J. M. Klein Gebbink, *J. Am. Chem. Soc.*, 2007, **129**, 2275.
149 S. Tanase and E. Bouwman, *Adv. Inorg. Chem.*, 2006, **58**, 29.
150 Y.-M. Chiou and L. Que, Jr, *J. Am. Chem. Soc.*, 1995, **117**, 3999.
151 E. H. Ha, R. Y. N. Ho, J. F. Kisiel and J. S. Valentine, *Inorg. Chem.*, 1995, **34**, 2265.
152 S. Hikichi, T. Ogihara, K. Fujisawa, N. Kitajima, M. Akita and Y. Moro-oka, *Inorg. Chem.*, 1997, **36**, 4539.
153 M. P. Mehn, K. Fujisawa, E. L. Hegg and L. Que, Jr, *J. Am. Chem. Soc.*, 2003, **125**, 7828.
154 T. K. Paine, H. Zheng and L. Que, Jr, *Inorg. Chem.*, 2005, **44**, 474.
155 T. K. Paine, J. England and L. Que, Jr, *Chem.–Eur. J.*, 2007, **13**, 6073.
156 M. P. Jensen, S. J. Lange, M. P. Mehn, E. L. Que and L. Que, Jr, *J. Am. Chem. Soc.*, 2003, **125**, 2113.
157 Y. Mekmouche, S. Menage, C. Toia-Duboc, M. Fontecave, J.-B. Galey, C. Lebrun and J. Pecaut, *Angew. Chem., Int. Ed.*, 2001, **40**, 949.
158 A. Nielsen, F. B. Larsen, A. D. Bond and C. J. McKenzie, *Angew. Chem., Int. Ed.*, 2006, **45**, 1602.
159 N. Y. Oh, M. S. Seo, M. H. Lim, M. B. Consugar, M. J. Park, J.-U. Rohde, J. Han, K. M. Kim, J. Kim, L. Que, Jr and W. Nam, *Chem. Commun.*, 2005, 5644.
160 S. Taktak, M. Flook, B. M. Foxman, L. Que, Jr and E. V. Rybak-Akimova, *Chem. Commun.*, 2005, 5301.
161 R. Yamahara, S. Ogo, H. Masuda and Y. Watanabe, *J. Inorg. Biochem.*, 2002, **88**, 284.
162 T. Funabiki, A. Mizoguchi, T. Sugimoto, S. Tada, M. Tsuji, H. Sakamoto and S. Yoshida, *J. Am. Chem. Soc.*, 1986, **108**, 2921.
163 D.-H. Jo, Y.-M. Chiou and L. Que, Jr, *Inorg. Chem.*, 2001, **40**, 3181.
164 G. Lin, G. Reid and T. D. H. Bugg, *J. Am. Chem. Soc.*, 2001, **123**, 5030.
165 A. Dei, D. Gatteschi and L. Pardi, *Inorg. Chem.*, 1993, **32**, 1389.
166 D.-H. Jo and L. Que, Jr, *Angew. Chem., Int. Ed.*, 2000, **39**, 4284.
167 T. Ogihara, S. Hikichi, M. Akita and Y. Moro-oka, *Inorg. Chem.*, 1998, **37**, 2614.
168 G. Lin, G. Reid and T. D. H. Bugg, *Chem. Commun.*, 2000, 1119.

169 N. Raffard, R. Carina, A. J. Simaan, J. Sainton, E. Riviere, L. Tchertanov, S. Bourcier, G. Bouchoux, M. Delroisse, F. Banse and J.-J. Girerd, *Eur. J. Inorg. Chem.*, 2001, 2249.
170 P. D. Oldenburg and L. Que, Jr, *Catal. Today*, 2006, **117**, 15.
171 K. Chen and L. Que, Jr, *Angew. Chem., Int. Ed.*, 1999, **38**, 2227.
172 M. Costas, A. K. Tipton, K. Chen, D.-H. Jo and L. Que, Jr, *J. Am. Chem. Soc.*, 2001, **123**, 6722.
173 R. Mas-Balleste, M. Costas, T. van den Berg and L. Que, Jr, *Chem.–Eur. J.*, 2006, **12**, 7489.
174 A. Bassan, M. R. A. Blomberg, P. E. M. Siegbahn and L. Que, Jr, *Angew. Chem., Int. Ed.*, 2005, **44**, 2939.
175 D. Quinonero, K. Morokuma, D. Musaev, R. Mas-Balleste and L. Que, Jr, *J. Am. Chem. Soc.*, 2005, **127**, 6548.
176 M. Fujita, M. Costas and L. Que, Jr, *J. Am. Chem. Soc.*, 2003, **125**, 9912.
177 M. Klopstra, G. Roelfes, R. Hage, R. M. Kellogg and B. L. Feringa, *Eur. J. Inorg. Chem.*, 2004, 846.
178 P. D. Oldenburg, A. A. Shteinman and L. Que, Jr, *J. Am. Chem. Soc.*, 2005, **127**, 15672.
179 O. Rotthaus, S. Le Roy, A. Tomas, K. M. Barkigia and I. Artaud, *Inorg. Chim. Acta*, 2004, **357**, 2211.
180 M. R. Bukowski, P. Comba, A. Lienke, C. Limberg, C. Lopez de Laorden, R. Mas-Balleste, M. Merz and L. Que, Jr, *Angew. Chem., Int. Ed.*, 2006, **45**, 3446.
181 M. S. Chen and M. C. White, *Science*, 2007, **318**, 783.
182 G. Katona, P. Carpentier, V. Niviere, P. Amara, V. Adam, J. Ohana, N. Tsanov and D. Bourgeois, *Science*, 2007, **316**, 449.
183 R. J. Guajardo, S. E. Hudson, S. J. Brown and P. K. Mascharak, *J. Am. Chem. Soc.*, 1993, **115**, 7971.
184 G. Roelfes, V. Vrajmasu, K. Chen, R. Y. N. Ho, J.-U. Rohde, C. Zondervan, R. M. la Crois, E. P. Schudde, M. Lutz, A. L. Spek, R. Hage, B. L. Feringa, E. Munck and L. Que, Jr, *Inorg. Chem.*, 2003, **42**, 2639.
185 R. Y. N. Ho, G. Roelfes, B. L. Feringa and L. Que, Jr, *J. Am. Chem. Soc.*, 1999, **121**, 264.
186 A. Wada, S. Ogo, S. Nagamoto, T. Kitagawa, Y. Watanabe, K. Jitsukawa and H. Masuda, *Inorg. Chem.*, 2002, **41**, 616.
187 A. Hazell, C. J. McKenzie, L. P. Nielsen, S. Schindler and M. Weitzer, *J. Chem. Soc., Dalton Trans.*, 2002, 310.
188 M. R. Bukowski, P. Comba, C. Limberg, M. Merz, L. Que, Jr and T. Wistuba, *Angew. Chem., Int. Ed.*, 2004, **43**, 1283.
189 J.-J. Girerd, F. Banse and A. J. Simaan, *Struct. Bonding*, 2000, **97**, 145.
190 K. D. Koehntop, J.-U. Rohde, M. Costas and L. Que, Jr, *Dalton Trans.*, 2004, 3191.
191 A. J. Simaan, S. Dopner, F. Banse, S. Bourcier, G. Bouchoux, A. Boussac, P. Hildebrandt and J.-J. Girerd, *Eur. J. Inorg. Chem.*, 2000, 1627.
192 K. Hashimoto, S. Nagatomo, S. Fujinami, H. Furutachi, S. Ogo, M. Suzuki, A. Uehara, Y. Maeda, Y. Watanabe and T. Kitagawa, *Angew. Chem., Int. Ed.*, 2002, **41**, 1202.
193 H. Furutachi, K. Hashimoto, S. Nagatomo, T. Endo, S. Fujinami, Y. Watanabe, T. Kitagawa and M. Suzuki, *J. Am. Chem. Soc.*, 2005, **127**, 4550.
194 K. B. Jensen, C. J. McKenzie, L. P. Nielsen, J. Z. Pedersen and H. M. Svendsen, *Chem. Commun.*, 1999, 1313.
195 R. Y. N. Ho, G. Roelfes, R. Hermant, R. Hage, B. L. Feringa and L. Que, Jr, *Chem. Commun.*, 1999, 2161.
196 M. J. Park, J. Lee, Y. Suh, J. Kim and W. Nam, *J. Am. Chem. Soc.*, 2006, **128**, 2630.
197 J. Annaraj, Y. Suh, M. S. Seo, S. O. Kim and W. Nam, *Chem. Commun.*, 2005, 4529.
198 L. Que, Jr, *Acc. Chem. Res.*, 2007, **40**, 493.
199 C. A. Grapperhaus, B. Mienert, E. Bill, T. Weyhermuller and K. Wieghardt, *Inorg. Chem.*, 2000, **39**, 5306.
200 A. Decker, M. D. Clay and E. I. Solomon, *J. Inorg. Biochem.*, 2006, **100**, 697.
201 A. Decker, J.-U. Rohde, L. Que, Jr and E. I. Solomon, *J. Am. Chem. Soc.*, 2004, **126**, 5378.
202 C. V. Sastri, M. J. Park, T. Ohta, T. A. Jackson, A. Stubna, M. S. Seo, J. Lee, J. Kim, T. Kitagawa, E. Munck, L. Que, Jr and W. Nam, *J. Am. Chem. Soc.*, 2005, **127**, 12494.
203 J.-U. Rohde, S. Torelli, X. Shan, M. H. Lim, E. J. Klinker, J. Kaizer, K. Chen, W. Nam and L. Que, Jr, *J. Am. Chem. Soc.*, 2004, **126**, 16750.
204 J.-U. Rohde, A. Stubna, E. L. Bominaar, E. Munck, W. Nam and L. Que, Jr, *Inorg. Chem.*, 2006, **45**, 6435.
205 J.-U. Rohde and L. Que, Jr, *Angew. Chem., Int. Ed.*, 2005, **44**, 2255.
206 M. Martinho, F. Banse, J.-F. Bartoli, T. A. Mattioli, P. Battioni, O. Horner, S. Bourcier and J.-J. Girerd, *Inorg. Chem.*, 2005, **44**, 9592.
207 C. V. Sastri, K. Oh, Y. J. Lee, M. S. Seo, W. Shin and W. Nam, *Angew. Chem., Int. Ed.*, 2006, **45**, 3992.
208 M. S. Seo, J.-H. In, S. O. Kim, N. Y. Oh, J. Hong, J. Kim, L. Que, Jr and W. Nam, *Angew. Chem., Int. Ed.*, 2004, **43**, 2417.
209 M. H. Lim, J.-U. Rohde, A. Stubna, M. R. Bukowski, M. Costas, R. Y. N. Ho, E. Munck, W. Nam and L. Que, Jr, *Proc. Natl. Acad. Sci. U. S. A.*, 2003, **100**, 3665.
210 M. P. Jensen, M. Costas, R. Y. N. Ho, J. Kaizer, A. Mairata i Payeras, E. Munck, L. Que, Jr, J.-U. Rohde and A. Stubna, *J. Am. Chem. Soc.*, 2005, **127**, 10512.
211 S. O. Kim, C. V. Sastri, M. S. Seo, J. Kim and W. Nam, *J. Am. Chem. Soc.*, 2005, **127**, 4178.
212 J. Kaizer, M. Costas and L. Que, Jr, *Angew. Chem., Int. Ed.*, 2003, **42**, 3671.
213 O. Pestovsky, S. Stoian, E. L. Bominaar, X. Shan, E. Munck, L. Que, Jr and A. Bakac, *Angew. Chem., Int. Ed.*, 2005, **44**, 6871.
214 J. Bautz, M. R. Bukowski, M. Kerscher, A. Stubna, P. Comba, A. Lienke, E. Munck and L. Que, Jr, *Angew. Chem., Int. Ed.*, 2006, **45**, 5681.
215 W. Nam, *Acc. Chem. Res.*, 2007, **40**, 522.
216 J. Kaizer, E. J. Klinker, N. Y. Oh, J.-U. Rohde, W. J. Song, A. Stubna, J. Kim, E. Munck, W. Nam and L. Que, Jr, *J. Am. Chem. Soc.*, 2004, **126**, 472.
217 N. Y. Oh, Y. Suy, M. J. Park, M. S. Seo, J. Kim and W. Nam, *Angew. Chem., Int. Ed.*, 2005, **44**, 4235.
218 C. V. Sastri, M. S. Seo, M. J. Park, K. M. Kim and W. Nam, *Chem. Commun.*, 2005, 1405.
219 K. Nehru, M. S. Seo, J. Kim and W. Nam, *Inorg. Chem.*, 2007, **46**, 293.
220 D. Kumar, H. Hirao, L. Que, Jr and S. Shaik, *J. Am. Chem. Soc.*, 2205, **127**, 8026.
221 K. Chen and L. Que, Jr, *J. Am. Chem. Soc.*, 2001, **123**, 6327.
222 N. Aliaga-Alcalde, S. DeBeer George, B. Mienert, E. Bill, K. Wieghardt and F. Neese, *Angew. Chem., Int. Ed.*, 2005, **44**, 2908.
223 K. Meyer, E. Bill, B. Mienert, T. Weyhermuller and K. Wieghardt, *J. Am. Chem. Soc.*, 1999, **121**, 4859.
224 S. S. Gupta, M. Stadler, C. A. Noser, A. Ghosh, B. Steinhoff, D. Lenoir, C. P. Horwitz, K.-W. Schramm and T. J. Collins, *Science*, 2002, **296**, 326.
225 T. J. Collins, *Acc. Chem. Res.*, 2002, **35**, 782.

